

Spin State Energetics in First-Row Transition Metal Complexes: Contribution of (3s3p) Correlation and its Description by Second-Order Perturbation Theory

Kristine Pierloot,^{*} Quan Manh Phung, and Alex Domingo

Department of Chemistry, KU Leuven, Celestijnenlaan 200F, B-3001 Leuven, Belgium

E-mail: kristin.pierloot@chem.kuleuven.be

^{*}To whom correspondence should be addressed

Abstract

This paper presents an in-depth study of the performance of multiconfigurational second-order perturbation theory (CASPT2, NEVPT2) in describing spin state energetics in first row transition metal (TM) systems, including bare TM ions, TM ions in a field of point charges (TM/PC), and an extensive series of TM complexes, where the main focus lies on the (3s3p) correlation contribution to the relative energies of different spin states. To the best of our knowledge, this is the first systematic NEVPT2 investigation of TM spin state energetics. CASPT2 has been employed in several previous studies, but was regularly found to be biased towards high spin states. The bias was attributed to a too low value of the so-called IPEA shift ϵ , an empirical correction in the CASPT2 zeroth-order Hamiltonian with a standard value of 0.25 hartree. Based on comparisons with experiment (TM ions) and calculations with the multireference configuration interaction (TM ions and TM/PC systems) and coupled-cluster (TM complexes) methods, we demonstrate in this work that standard CASPT2 works well for valence correlation and that its bias towards high-spin states is caused by an erratic description of (3s3p) correlation effects. The latter problem only occurs for spin transitions involving a ligand field (de)excitation, not in bare TM ions. At the same time the (3s3p) correlation contribution also becomes strongly ϵ dependent. The error can be reduced by increasing ϵ , but only at the expense of deteriorating the CASPT2 description of valence correlation in the TM complexes. The alternative NEVPT2 method works well for bare TM and TM/PC systems, but its results for the TM complexes are disappointing, with large errors both for the valence and (3s3p) correlation contributions to the relative energies of different spin states.

Introduction

In transition metal (TM) complexes, different spin states may play a central role in enzymatic reactions and their biomimetic analogues, in spin crossover phenomena, as well as in industrial catalysis. The accurate description of TM spin state energetics, that is the relative energies of alternative spin states, has proven to be an exceedingly difficult problem for quantum chemistry methods. In particular, density functional theory (DFT), still the method of choice in most computational studies, has failed to provide a reliable and systematic high accuracy, by predicting relative energies that strongly vary (by tens of kcal/mol) between different exchange-correlation functionals.¹⁻⁶ The growing awareness that DFT might be at its wits end over this problem, combined with a series of novel developments in hardware, algorithms and reduced scaling approaches⁷⁻¹⁵ have certainly brought alternative methods based on ab initio wave function theory (WFT) back into the picture. Wave function-based ab initio calculations generally proceed in two steps: the calculation of the reference (zeroth order) wave function and the subsequent calculation of the dynamic correlation energy. In single reference methods the reference wave function is chosen to be a single Slater determinant, while multireference methods start from a multi-determinant wave function. To treat dynamic correlation, coupled-cluster (CC) theory undoubtedly is the most accurate method available, and CCSD(T) (including single, double, and perturbative triple excitations)^{16,17} is often referred to as the “gold standard” in WFT. However, because of its high computational cost, CCSD(T) calculations are generally only affordable in a single reference approach. A recent article from Radoń et al.¹⁸ offers highly accurate CCSD(T) results, extrapolated to the basis set limit, of the spin state energetics of TM heme and heme-related systems. Unfortunately, the largest systems that could be treated with this approach are the highly symmetric heme systems FeP and FePCl (P = porphyrin). A much cheaper alternative for treating dynamic correlation is second-order perturbation theory. Cheaper of course might also mean lower accuracy, but this may be circumvented by moving to a multireference approach which treats the most important correlation effects (static correlation as well as the so-called 3d double shell effect in first-row TM) already in the reference wave function. Multiconfigurational perturbation theory based on a complete active

space reference wave function (CASSCF/CASPT2)^{19,20} so far has been the most commonly used multireference approach for large TM complexes, including several studies on spin state energetics. In CASPT2, the zeroth-order Hamiltonian is based on a generalized Fock type operator (see further below). A more elaborate zeroth-order Hamiltonian, including also two-electron terms, has been proposed in the NEVPT2 scheme (NEV = *n*-electron valence).²¹ However, to the best of our knowledge, NEVPT2 has so far not been employed in any (systematic) study of spin state energetics in TM complexes. Alternatively, the CASSCF reference wave function can be replaced by a RASSCF (Restricted Active Space SCF)²² DMRG (Density Matrix Renormalization Group),^{23–26} or FCIQMC-CASSCF (Full Configuration Interaction Quantum Monte Carlo CASSCF)¹¹ wave function. The latter methods have the advantage that more molecular orbitals can be involved in the active space from which the reference wave function is built.

In many cases, the accuracy obtained from CASPT2 for spin state energetics in TM complexes is satisfactory.^{4–6,27} However, it was also reported on several occasions that CASPT2 favors high-spin over low-spin states, with errors up to 0.3–0.5 eV.^{6,28–33} As the error is systematically in favor of high-spins, it has been attributed^{31–33} to an inadequate formulation of the zeroth-order order Hamiltonian in CASPT2, in particular to the value of the so-called IPEA shift, introduced in the CASPT2 method in 2004 by Ghigo et al.³⁴

Originally, the zeroth-order Hamiltonian in CASPT2 was based on the following simple (generalized) one-electron Fock matrix F ²⁰

$$F_{pq} = h_{pq} + \sum_{r,s} D_{rs} \left((pq|rs) - \frac{1}{2}(ps|rq) \right) \quad (1)$$

The diagonal elements of F correspond to $-\text{IP}$ (IP = ionization potential) for the inactive orbitals, to $-\text{EA}$ (EA = electron affinity) for the virtual orbitals, whereas they would be a weighted average of $-\text{IP}$ and $-\text{EA}$ for the active orbitals. This original formulation, however, leads to denominators in the expression for the second-order energy that are too small in the case of excitations into or out of a partially occupied orbital. As a result, the perturbation energy of open shell systems was

overestimated, with an error that increases with the number of unpaired electrons.^{35,36} In ref. 34 a simple remedy was proposed, consisting of a downward shift of the diagonal Fock matrix elements towards $-IP$ for an orbital that is excited out of and an upward shift toward $-EA$ for an orbital that is excited into. Applying this so-called IPEA shift leads to a more balanced description of states with a different number of unpaired electrons. But obviously, the relative CASPT2 energy of such states becomes dependent on the value of the applied shift, where larger shifts lead to a relative stabilization of low spin with respect to high spin states. A standard IPEA shift of 0.25 hartree was proposed in ref. 34, based on test calculations on the binding energies of a series of diatomic molecules (built from main group atoms from the first, second, and third row of the periodic table up to Br), and on excitation energies in N_2 and benzene. As of 2006, this IPEA-shifted CASPT2 became the standard in the MOLCAS software.

However, for a number of first-row transition metal systems it was reported that even the IPEA-shifted CASPT2 leads to a (more or less) systematic overstabilization of high- with respect to low-spin states. This analysis almost naturally led to the suggestion of increasing the IPEA shift for a more accurate description of this property. Unfortunately, benchmarking studies on TM in different environments and oxidation states have not reached a consensus concerning a common single value of IPEA that would systematically improve the description of spin state energetics in *all* (or at least first-row) transition metal complexes in their different oxidation states. Indeed, values of IPEA ranging between 0.25 hartree (the standard) and as large as 1.5 hartree have been suggested for different complexes.^{6,27,31–33}

In order to approach highly accurate spin state energetics for first-row TM systems, another factor to be considered carefully concerns the correlation of the metal semi-core (3s3p) electrons. This was proven already in an early CASPT2 benchmarking paper on the multiplet splittings in TM ions,³⁷ showing that including (3s3p) correlation in the perturbation treatment may profoundly (by up to 0.5 eV) affect the relative term energies. The importance of (3s3p) correlation in TM complexes was also illustrated in studies of electronic spectra^{38,39} and metal-ligand binding energies.^{40,41} In a recent RASPT2 investigation of the spin state energetics of FeP^{42} it was shown

that in order to obtain the correct triplet (rather than quintet) ground state for this molecule, it is necessary to also include the (3s3p) orbitals next to selected valence orbitals in a large active space. As we will show below, the good result for the quintet-triplet splitting presented in that work may have been fortuitous (see below and Table 4), but it proves that (3s3p) correlation is indeed also important for spin state energetics and deserves proper attention when aiming for high accuracy in correlated wave function calculations on TM systems.

This paper presents a profound investigation of (3s3p) correlation effects on the relative energies of different spin states of a given $3d^n$ configuration in first-row TM systems, aiming at providing a clear estimate of the expected accuracy from multiconfigurational second-order perturbation theory PT2. The role of the zeroth-order Hamiltonian is investigated by comparing CASPT2 results with varying IPEA shifts, and the results from CASPT2 with NEVPT2. This investigation is performed for three relevant series of TM systems: (a) bare metal cations with different oxidation states, (b) metal cations surrounded by point charges (TM/PC), (c) a broad series of relevant TM complexes, shown in Figure 1: $M^{II}P$ and $M^{II}L_2$, with $M = Mn, Fe, Co$; P standing for porphyrin; and L for the bidentate, N-donor ligand $C_3N_2H_5^-$. ML_2 has been considered as a simplified mimic for the full MP heme in earlier coupled-cluster studies.^{6,18,43} The following five- and six-coordinated ferric heme systems and their L_2 mimics were also included: $Fe^{III}L_2(OH)$ and $Fe^{III}P(OH)$, $Fe^{III}L_2(NH_3)(OH)$ and $Fe^{III}P(NH_3)(OH)$, $Fe^{III}L_2(SH)$ and $Fe^{III}P(SH)$. Our study also includes two weak-field octahedral complexes $[M^{II}(NCH)_6]^{2+}$ ($M = Fe, Co$), that were the subject of a previous performance tests of the CASPT2 zeroth-order Hamiltonian.³² Two organometallic complexes were also considered: $Mn(Cp)_2$ and $Ni(Cp)(acac)$ ($Cp =$ cyclopentadienyl, $acac =$ acetylacetonate). The (3s3p) correlation contributions obtained from PT2 are benchmarked against either CCSD(T) (for strong-field TM complexes) or MRCI (for free TMs and TMs with point charges) calculations.

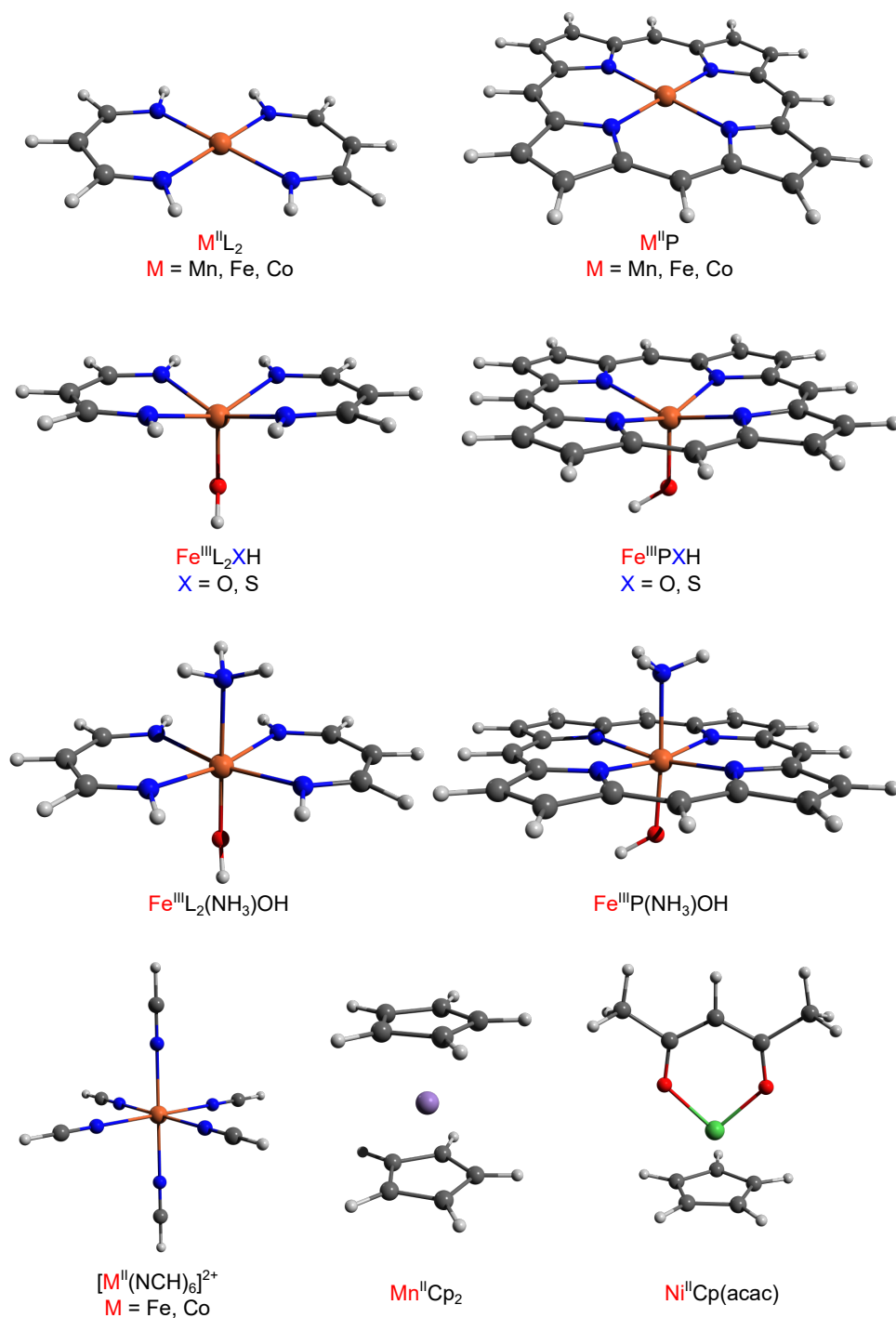


Figure 1: Transition metal complexes studied in this work

Computational Details

The active spaces used in the multiconfigurational perturbation theory calculations are the same for CASPT2 and NEVPT2 in all cases, and are built according to the standard rules for transition

metal complexes.^{28,42,44–46} Calculations on the metal ions (bare or surrounded by point charges) were performed with an active space of either five (3d) or ten (3d,4d) orbitals, where the 4d shell serves to describe the metal 3d double-shell correlation effect. Including this (essentially dynamic) correlation effect in the reference wave function is deemed to be important only when the second step in the correlation treatment is treated with second-order perturbation theory (PT2), not when configuration-interaction (CI) is used instead (as the results for the TM ions will confirm). Therefore, all MRCI calculations on the metal ions were based on an active space including only the five metal 3d orbitals.

The (3d,4d) shells were present in the active space of all molecular PT2 calculations, which also includes important ligand orbitals involved in covalent interactions with the metal 3d orbitals. With $CAS(n_e, n_o)$ denoting an active space of n_e electrons in n_o orbitals, the four-coordinated complexes $M^{II}P$ and $M^{II}L_2$ are described with a $CAS(7,11)$ ($M = Co$), $CAS(8,11)$ ($M = Fe$) and $CAS(9,11)$ ($M = Co$) space, including the $M(3d,4d)$ and one additional σ -type bonding orbital on the porphyrin N donor atoms. For the $Fe^{III}L_2(SH)$ and $Fe^{III}P(SH)$ complexes, two extra bonding orbitals, predominantly SH (σ, π), were included in the active space giving $CAS(11,13)$. For the corresponding OH complexes, this active space was extended to $CAS(11,15)$, including two extra orbitals with predominant oxygen 3p character. This is necessary because the fully occupied O 2p shell in OH^- gives rise to a 2p double-shell effect that is (energetically) more important than the metal 3d double-shell effect, such that in an active space with only 13 active orbitals, two M 4d orbitals are rotated into O 3p. Note that the same phenomenon does not occur for S 3p. No NH_3 orbitals were included in the active space of $Fe^{III}L_2(OH)(NH_3)$ and $Fe^{III}P(OH)(NH_3)$, as the $M-NH_3$ bond was found to be very ionic. The two pseudo-octahedral complexes $[Fe(NCH)_6]^{2+}$ and $[Co(NCH)_6]^{2+}$ were described with a $CAS(10,12)$ and $CAS(11,12)$ active space, containing next to $M(3d,4d)$ two σ -type orbitals on the N donor ligands (corresponding to the octahedral e_g σ orbitals). The two organometallic compounds also contain a number of π^* orbitals in their active space. For $Mn(Cp)_2$ (D_{5h}) a $CAS(9,14)$ space was used containing, next to $Mn(3d,4d)$, the Cp $e_1''(\pi)$ and $e_2'(\pi^*)$ shells.⁴⁷ $Ni(Cp)(acac)$ (C_s) was described with a $CAS(14,15)$ space, containing the same Cp (π, π^*) set of

orbitals as well as an acac σ orbital. A plot of the active orbitals of the Ni(Cp)(acac) complex is included in the Supporting Information (SI, Figure S1). It should be mentioned that for the low-spin states, where one or two of the metal 3d orbitals are unoccupied, the corresponding 4d orbitals were removed from the active space in cases where they would otherwise become strongly mixed with (or completely rotated into) other virtual orbitals.

Test calculations for FeP were performed with two extended active spaces including (a) the (3s3p) orbitals to give a (16,15) space, and (b) further extending it with (4s4p) to give a (16,19) space. With the latter active space CASSCF calculations become prohibitively large. The CASSCF formalism was therefore replaced by either RASSCF²² (with (3s3p) in RAS1, (4s4p) in RAS3, and allowing up to quadruple excitations out of RAS1 and into RAS3) or DMRG^{23–26} (using 1500 renormalized states). The choice of these parameters is based on extensive benchmarking of RASPT2⁴² and DMRG/CASPT2,⁴⁸ and are expected to give PT2 relative energies that approach the full CASPT2 result to within 1 kcal/mol.

All calculations denoted as C(R)ASPT2 use the default IPEA shift ($\epsilon = 0.25$ hartree) for the zeroth-order Hamiltonian H^0 .³⁴ We also performed CASPT2 calculations with other ϵ values, ranging between 0.0 and 2.0 hartree in steps of 0.25 hartree, to investigate the influence of the IPEA shift in H^0 . In cases where the value of the CASPT2 IPEA shift was varied, this is explicitly mentioned in the text/tables. A small imaginary level shift⁴⁹ of 0.1 hartree was also used in all CASPT2 calculations to improve the convergence of the iterative procedure and to circumvent intruder states. All NEVPT2 calculations were performed using the PC-NEVPT2⁵⁰ (partially contracted n -electron valence state perturbation theory) formalism. All CCSD(T) calculations are (partially) spin restricted, based on restricted open-shell ROHF orbitals.^{16,17} Also note that all reported MRCI energies are Davidson corrected.

Structures of the molecules are shown in Figure 1. In most cases, they were taken from previous studies, where they were optimized separately for each spin state. For the ML₂ and MP molecules we made use of the structures available from Radoń's paper¹⁸ (DFT structures optimized with BP86 and def2-TZVP basis sets), except for FeP, for which we used the PBE0 optimized struc-

tures that we also used in our previous RASPT2 study.⁴² For the ferric complexes $\text{Fe}^{\text{III}}\text{L}_2(\text{SH})$ and $\text{Fe}^{\text{III}}\text{P}(\text{SH})$, BP86 structures were also taken from ref. 18. Note that for all L_2 systems, the necessary constraints were imposed on the structures in order to keep the planar arrangement of the four nitrogen atoms (to resemble the metal ligation by porphyrin). Structures for the ferric porphyrin systems with axial OH were obtained in this work, using exactly the same procedure as used previously by Radón. The structures of the $[\text{M}(\text{NCH}_6)]^{2+}$ complexes were taken from ref. 32. They were obtained there with the OLYP functional, using (Slater type) basis sets of TZP quality. For $\text{Mn}(\text{Cp})_2$, we used structures from our previous work on metallocene binding energies⁴⁷ (PBE0 with def2-TZVP basis sets). Finally, for $\text{Ni}(\text{Cp})(\text{acac})$, structures for both spin states were obtained in this work, using the BP86 functional and def2-TZVP basis sets. For convenience, the structures (Cartesian coordinates) of all molecules studied in this work are provided in the SI.

All calculations on the free metal ions were performed without symmetry. Proper atomic symmetry is obtained in CASSCF by optimizing a set of average orbitals for the different terms belonging to a given multiplet. All calculations on the metal ions surrounded by point charges (PC) were performed using D_{2h} symmetry, even though the actual symmetry of these systems is either O_h (six PC) or D_{4h} (four PC). This means that symmetry breaking may occur for states that would be degenerate in the parent O_h or D_{4h} symmetry. The principal configuration(s) of all calculated states of the TM/PC systems are given in Table S1. For the molecules, extra information on the symmetry point group and positioning in the coordinate system is also provided in the SI (Table S2).

All C(R)ASPT2 and MRCI calculations were performed with MOLCAS v7.9,⁵¹ whereas NEVPT2 and CCSD(T) calculations were performed with the MOLPRO 2009⁵² package. For the DMRG calculation on FeP we made use of the CHEMPS2 program⁵³ interfaced with MOLCAS v8.1.⁵⁴ The same ANO-RCC basis sets were used in all these correlated wave function calculations, with the following contractions: [7s6p5d3f2g1h] for the metals,⁵⁵ [4s3p2d1f] for C, N, O,^{56,57} [5s4p3d2f] for S, and [3s1p] for H.⁵⁸ The ANO-rcc basis sets were designed to include relativistic effects and to provide an accurate description of semicore (3s3p) correlation in first-row TM

systems. Scalar relativistic effects were included using the standard 2nd-order Douglas-Kroll-Hess Hamiltonian.⁵⁹ In the CASPT2 calculations (but not in NEVPT2, MRCI, and CC) the two-electron integrals were approximated with the Cholesky decomposition technique, using a threshold of 10^{-6} hartree.^{60,61} DFT geometry optimizations, where needed, were performed with the TURBOMOLE v6.4⁶² program, making use of def2-TZVP basis sets.⁶³

Results and Discussion

Effect of (3s3p) correlation on the spin state energetics in bare TM ions

To start this investigation, we decided to consider first the spin state energetics in a number of relevant bare TM ions: Mn^{2+} (d^5), Fe^{3+} (d^5), Fe^{2+} (d^6), Co^{2+} (d^7), and Ni^{2+} (d^8). For each of these ions the lowest states of different spin multiplicities were considered: the high-spin ground state, and one or two excited states where the total spin is lowered by one or (if possible) by two units. These calculations were performed with MRCI, CASPT2, and NEVPT2. The results are shown in Table 1, including also the experimental data taken from ref. 64 – 67 (as a weighted average of the different J terms). The table shows the results for the spin transition energies obtained from calculations that either do or do not include the eight electrons from the metal 3s and 3p orbitals in the second-order perturbation treatment, indicated as +sp and *nosp* respectively. In the following discussion, the first correlation treatment will be denoted as ‘full correlation’, the latter as ‘valence correlation’. The difference between the relative energies obtained from both sets of calculations is referred to as the (3s3p) correlation effect, and is denoted as Δ_{sp} in Table 1.

For NEVPT2 and CASPT2 two different active spaces were used, including only the five 3d orbitals: $\text{CAS}(n_e,5)$, or including an extra d shell describing the 3d double-shell effect: $\text{CAS}(n_e,10)$ (n_e being the occupation number of the 3d shell). Both sets of results quite closely agree, indicating that the double-shell effect is limited for transitions within the 3d-shell of these bare TM ions. For the d^5 ions Mn^{2+} and Fe^{3+} hardly any difference (< 1 kcal/mol) is found between the PT2 results based on the (5,5) and (5,10) active spaces. Conversely, for d^6 – d^8 ions the effect becomes more

Table 1: Spin state energetics in atomic ions: Relative spin states energy ΔE (kcal/mol) obtained from different computational approaches for states with total spin decreased by one or two units with respect to the high spin ground state

	MRCI($n_e,5$)	NEVPT2($n_e,5$)	NEVPT2($n_e,10$)	CASPT2($n_e,5$) ^a	CASPT2($n_e,10$) ^a	Exp. ^b	
Mn²⁺ ($n_e = 5$)							
⁶ S→ ⁴ G	$\Delta E(nosp)$	84.1	84.6	83.9	83.5(+0.6)	83.9(+0.3)	76.8
	$\Delta E(+sp)$	77.7	77.4	77.0	78.6(+0.3)	78.9(+0.4)	
	Δ_{sp}	-6.4	-7.2	-6.9	-4.9(-0.3)	-5.0(+0.1)	
⁶ S→ ² I	$\Delta E(nosp)$	122.6	122.5	121.8	121.8(+1.0)	122.2(+0.6)	112.1
	$\Delta E(+sp)$	114.2	111.5	111.2	115.3(+0.4)	115.5(+0.5)	
	Δ_{sp}	-8.4	-11.0	-10.6	-6.5(-0.6)	-6.7(-0.1)	
Fe³⁺ ($n_e = 5$)							
⁶ S→ ⁴ G	$\Delta E(nosp)$	100.3	100.4	100.0	99.7(+0.2)	100.1(+0.2)	92.2
	$\Delta E(+sp)$	93.8	93.1	93.0	94.8(-0.1)	95.1(+0.5)	
	Δ_{sp}	-6.5	-7.3	-7.0	-4.9(-0.3)	-5.0(+0.3)	
⁶ S→ ² I	$\Delta E(nosp)$	145.7	145.4	144.9	145.2(+0.8)	145.4(+0.5)	134.7
	$\Delta E(+sp)$	137.5	134.3	134.2	138.9(+0.3)	138.9(+0.5)	
	Δ_{sp}	-8.2	-11.1	-10.7	-6.3(-0.5)	-6.5(+0.0)	
Fe²⁺ ($n_e = 6$)							
⁵ D→ ³ P	$\Delta E(nosp)$	62.8	63.6	63.8	60.8(+3.1)	62.3(+1.2)	56.0
	$\Delta E(+sp)$	58.4	59.8	61.9	55.1(+6.3)	57.0(+4.4)	
	Δ_{sp}	-4.4	-3.8	-1.9	-5.7(+3.2)	-5.5(+3.2)	
⁵ D→ ¹ I	$\Delta E(nosp)$	93.7	92.2	92.4	91.7(+1.4)	92.7(+0.8)	85.6
	$\Delta E(+sp)$	87.8	83.7	84.7	86.3(+1.4)	87.3(+0.6)	
	Δ_{sp}	-5.9	-8.5	-7.7	-5.4(+0.0)	-5.5(-0.2)	
Co²⁺ ($n_e = 7$)							
⁴ F→ ² G	$\Delta E(nosp)$	51.8	50.8	51.2	48.5(+3.9)	50.9(+0.8)	47.3
	$\Delta E(+sp)$	48.4	47.3	48.5	44.4(+6.4)	47.4(+1.7)	
	Δ_{sp}	-3.4	-3.5	-2.7	-4.1(+2.5)	-3.5(+0.9)	
Ni²⁺ ($n_e = 8$)							
³ F→ ¹ D	$\Delta E(nosp)$	42.6	41.7	42.3	40.4(+1.4)	41.6(+0.8)	37.4
	$\Delta E(+sp)$	38.2	38.9	40.4	35.6(+0.8)	36.7(+1.1)	
	Δ_{sp}	-4.4	-2.8	-1.9	-4.8(-0.6)	-4.9(+0.3)	

^aThe numbers within parentheses are the slopes of the respective properties ($\delta\Delta E(nosp)$, $\delta\Delta E(+sp)$, $\delta\Delta_{sp}$) with respect to ϵ , as defined in eqs 2-3 (units are (kcal/mol)(hartree)⁻¹)

^btaken from ref. 64 – 67

significant, at least with CASPT2, with CASPT2($n_e,10$) predicting spin transition energies that are higher by up to 3 kcal/mol than CASPT2($n_e,5$). When considering Δ_{sp} , however, both sets of calculations differ by less than 1 kcal/mol in all cases. The rest of the discussion of the bare TM ions will be based on the CAS($n_e,10$) results.

As one can see, Δ_{sp} is always negative, ranging between -2 to -11 kcal/mol. Thus, the role of (3s3p) correlation is to stabilize states with lower spin with respect to higher spin states. Δ_{sp}

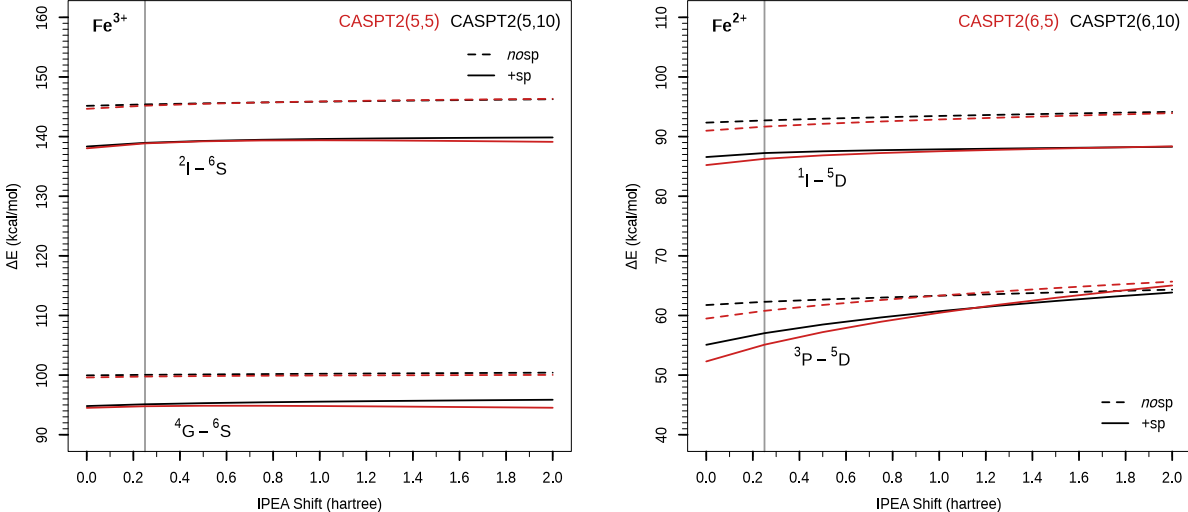


Figure 2: Spin state energetics in Fe^{3+} (left) and Fe^{2+} (right) as a function of the IPEA shift in the CASPT2 zeroth-order Hamiltonian.

is, in general, larger in absolute value when the total spin decreases by two units rather than one (although not twice as large). From the comparison of the calculated results to the experimental data in Table 1 it is clear that including (3s3p) in the correlation treatment is a prerequisite for predicting accurate spin state energetics in these ions. Without (3s3p) correlation, all calculated spin transition energies are considerably too high, whereas with (3s3p) correlation the error is reduced to at most 4 kcal/mol. Remaining errors with MRCI are systematically positive, and should mostly be attributed by insufficiencies in the TM basis set (see also the end of the discussion of the molecules). CASPT2(n_e ,10) also gives positive errors, while with NEVPT2 the errors in some cases become slightly negative. It is notable that in all cases the valence-only results obtained from NEVPT2(n_e ,10) and CASPT2(n_e ,10) agree with each other and with MRCI(n_e ,5) to within 1 kcal/mol. More pronounced differences between these methods are introduced by the treatment of (3s3p) correlation. The difference in Δ_{sp} between CASPT2 and MRCI is limited to at most 2 kcal/mol in all cases, but larger differences are found between CASPT2 and NEVPT2, e.g. 4 kcal/mol for the $^6S \rightarrow ^2I$ transition in the d^5 ions (with MRCI lying in between). This already points to a certain dependency of the PT2 description of (3s3p) correlation on the zeroth-order

Hamiltonian, although so far there are no systematic trends.

For CASPT2, it is also important to investigate how the perturbation treatment depends on the value of the IPEA shift ϵ in the zeroth-order Hamiltonian. To this end, full and valence only CASPT2 calculations were performed for ϵ ranging between 0.0 and 2.0 hartree. Figure 2 shows the curves obtained for the spin state transition energies as a function of ϵ for two representative cases, Fe^{3+} and Fe^{2+} . For Fe^{3+} , these curves are essentially flat, whereas the curves of Fe^{2+} , in particular the $^3\text{P}-^5\text{D}$ curve, show a positive slope that becomes even larger after including (3s3p) correlation. In order to simplify the discussion, a quantitative measure of the slope of the $\Delta E-\epsilon$ curves is defined as follows:

$$\delta\Delta E = \frac{4}{5} [\Delta E(\epsilon = 1.50 \text{ hartree}) - \Delta E(\epsilon = 0.25 \text{ hartree})] \quad (2)$$

Here, ΔE is the relative energy of a lower spin with respect to the highest spin state of the considered TM system. $\delta\Delta E$ corresponds to the slope of a linear $\Delta E - \epsilon$ curve which, as seen from Figure 2, is a reasonable approximation of the actual curves.

The values of $\delta\Delta E$ obtained according to equation 2 are given within parentheses in Table 1, next to the CASPT2 spin state energies resulting from the standard $\epsilon = 0.25$ hartree. Similarly, the dependence on ϵ of the (3s3p) correlation effect Δ_{sp} is given by:

$$\delta\Delta_{\text{sp}} = \frac{4}{5} [\Delta_{\text{sp}}(\epsilon = 1.50 \text{ hartree}) - \Delta_{\text{sp}}(\epsilon = 0.25 \text{ hartree})] \quad (3)$$

and is given within parentheses next to the standard CASPT2 value of Δ_{sp} for each state.

As one can see from these data, the valence CASPT2($n_e, 10$) relative energies in the bare ions are not significantly affected by the applied ϵ shift, showing curves with a slight positive slope of at most $1.3 \text{ (kcal/mol)(hartree)}^{-1}$. In most cases, this also remains true after (3s3p) correlation is included. Knowing that the IPEA shift was implemented in CASPT2 to avoid overstabilization of high spin with respect to low spin states, the expected behaviour with increasing ϵ would rather be opposite, i.e. negative slopes in all CASPT2 relative energies. Instead, the relative energies

obtained from full CASPT2 either are indifferent or slightly increase with ϵ , as for example the $^3\text{P}-^5\text{D}$ curve of Fe^{2+} (shown in Figure 2) and the $^2\text{G}-^4\text{F}$ curve of Co^{2+} . As the spin transition energies with full CASPT2 are already too high at $\epsilon = 0.25$ hartree, they can of course not benefit from a further increase in ϵ . On the contrary, a slight improvement might be obtained in most cases from CASPT2 calculations with the original zeroth-order Hamiltonian ($\epsilon = 0.0$ hartree). In the extreme case of the $^5\text{D}\rightarrow^3\text{P}$ transition in Fe^{2+} , the transition energy obtained with $\epsilon = 0.0$ hartree is 55.1 kcal/mol, 1.9 kcal/mol lower than with $\epsilon = 0.25$ hartree, and 0.9 kcal/mol lower than experiment.

However, on the whole these variations with ϵ are relatively minor, and we may conclude that the results obtained for the bare ions from the standard ($\epsilon = 0.25$ hartree) full CASPT2($n_e, 10$) calculations are satisfactory, close to both MRCI and experiment to within 4 kcal/mol.

Ions surrounded by point charges

We next consider what happens when these TM ions are surrounded by a set of point charges (PC), mimicking a (weak) crystal field. Either four or six point charges with charge (-0.5) were placed in a square planar or octahedral conformation around the metal. As in the previous section, calculations on the lowest state of different possible spin multiplicities were performed with CASPT2, NEVPT2 and MRCI, with and without including $(3s3p)$ in the dynamic correlation treatment. Representative results are collected in Table 2 (many other examples may be found in Tables S3–S5). All systems chosen in this Table are neutral, and the distances between the metal ion and the point charges were chosen such that the highest possible crystal field was obtained without the point charges actually intruding into the metal 3d shell. The resulting crystal field in these TM/PC systems is still much weaker than the ligand field of a real TM complex. This is manifested by the relative energies in Table 2, which all convincingly point to a high-spin ground state, although the states with lower spin are lowered in energy by 20-40 kcal/mol with respect to the free ions (Table 1).

As no experimental data are available for these systems, the MRCI results are used as a refer-

Table 2: Spin state energetics in ions surrounded by point charges: Relative spin state energy ΔE (kcal/mol) obtained from different computational approaches for states with total spin differing by one or two with respect to the high spin ground state

	MRCI($n_e,5$)	NEVPT2($n_e,5$)	NEVPT2($n_e,10$)	CASPT2($n_e,5$) ^a	CASPT2($n_e,10$) ^a	
Mn²⁺X₄^{-0.5} (1.2 Å) ($n_e = 5$)						
⁶ A _g → ⁴ B _{2g}	$\Delta E(nosp)$	43.1	45.0	43.7	47.0(-2.2)	44.3(-0.2)
	$\Delta E(+sp)$	40.1	41.4	40.8	47.6(-7.0)	45.2(-4.1)
	Δ_{sp}	-3.0	-3.6	-2.9	+0.6(-4.8)	+0.9(-3.9)
⁶ A _g → ² A _g	$\Delta E(nosp)$	80.9	81.9	81.1	86.6(-6.6)	82.7(-0.6)
	$\Delta E(+sp)$	77.1	78.0	77.8	90.7(-16.4)	86.3(-8.0)
	Δ_{sp}	-3.5	-3.9	-4.3	+4.1(-9.8)	+3.6(-7.4)
Fe³⁺X₆^{-0.5} (1.1 Å) ($n_e = 5$)						
⁶ A _g → ⁴ B _{1g}	$\Delta E(nosp)$	70.3	71.2	70.6	72.5(-1.1)	71.3(-0.2)
	$\Delta E(+sp)$	66.8	68.5	68.3	74.4(-5.4)	73.3(-3.9)
	Δ_{sp}	-3.5	-2.7	-7.2	+1.9(-4.3)	+2.0(-3.7)
⁶ A _g → ² A _g	$\Delta E(nosp)$	94.5	95.4	94.6	97.6(-3.4)	96.1(-0.6)
	$\Delta E(+sp)$	90.2	91.9	91.2	102.6(-12.7)	101.2(-8.2)
	Δ_{sp}	-4.3	-3.5	-3.4	+5.0(-9.3)	+5.1(-7.6)
Fe²⁺X₄^{-0.5} (1.2 Å) ($n_e = 6$)						
⁵ A _g → ³ B _{1g}	$\Delta E(nosp)$	50.2	45.6	48.0	47.9(-3.4)	48.7(-0.6)
	$\Delta E(+sp)$	44.0	43.2	47.1	50.2(-8.3)	51.3(-4.7)
	Δ_{sp}	-6.2	-2.4	-0.9	+2.3(-4.9)	+2.6(-4.1)
⁵ A _g → ³ B _{2g}	$\Delta E(nosp)$	50.3	44.4	47.6	47.3(-3.4)	48.3(-0.6)
	$\Delta E(+sp)$	43.7	42.4	46.8	49.3(-8.2)	50.6(-5.0)
	Δ_{sp}	-6.6	-2.0	-0.6	+2.0(-4.8)	+2.3(-4.4)
⁵ A _g → ¹ A _g	$\Delta E(nosp)$	82.6	75.6	79.5	81.2(-7.1)	81.1(-1.3)
	$\Delta E(+sp)$	76.3	74.9	80.7	87.6(-16.1)	87.3(-8.8)
	Δ_{sp}	-6.3	-0.7	+1.2	+6.4(-9.0)	+6.2(-7.5)
Co³⁺X₆^{-0.5} (1.1 Å) ($n_e = 6$)						
⁵ A _g → ³ B _{1g}	$\Delta E(nosp)$	49.6	49.6	49.5	51.3(-1.8)	50.5(-0.2)
	$\Delta E(+sp)$	46.1	47.1	46.9	52.6(-5.0)	52.6(-3.6)
	Δ_{sp}	-3.5	-2.5	-2.6	+2.3(-3.2)	+2.1(-3.4)
⁵ A _g → ¹ A _g	$\Delta E(nosp)$	58.1	57.4	57.6	61.1(-5.1)	59.6(-1.2)
	$\Delta E(+sp)$	57.2	57.9	58.3	69.6(-13.9)	67.8(-9.4)
	Δ_{sp}	-0.9	+0.5	+0.7	+8.5(-8.8)	+8.2(-8.2)
Co²⁺X₄^{-0.5} (1.2 Å) ($n_e = 7$)						
⁴ B _{1g} → ² A _g	$\Delta E(nosp)$	35.5	34.6	35.0	37.1(-3.9)	36.1(-0.9)
	$\Delta E(+sp)$	34.6	34.3	35.4	40.2(-8.1)	39.4(-4.6)
	Δ_{sp}	-0.9	-0.3	+0.4	+3.1(-4.2)	+3.3(-3.7)
Ni²⁺X₄^{-0.5} (1.1 Å) ($n_e = 8$)						
³ B _{3g} → ¹ A _g	$\Delta E(nosp)$	11.9	9.6	11.0	12.5(-5.1)	11.9(-1.3)
	$\Delta E(+sp)$	10.1	8.8	10.8	14.1(-8.1)	13.7(-4.9)
	Δ_{sp}	-1.8	-1.2	-0.2	+1.6(-3.0)	+1.8(-3.6)

^aThe numbers within parentheses are the slopes of the respective properties ($\delta\Delta E(nosp)$, $\delta\Delta E(+sp)$, $\delta\Delta_{sp}$) with respect to ϵ , as defined in eqs 2-3 (units are (kcal/mol)(hartree)⁻¹)

ence. Looking first at the results obtained from the valence only calculations (*nosp*), we again find good agreement between the results obtained from MRCI, NEVPT2($n_e,10$), and CASPT2($n_e,10$), where the double-shell effect is included in the reference wave function of the perturbational treatment. Differences between the three sets of results amount to at most 3 kcal/mol. The CASPT2($n_e,5$) results show a larger deviation, thus indicating the importance of including the second d-shell in the active space. We also note that the double-shell effect is somewhat less important (but not absent) in NEVPT2 as compared to CASPT2. From the close correspondence between CASPT2($n_e,10$) and MRCI we may conclude that the standard IPEA zeroth order Hamiltonian ($\epsilon = 0.25$ hartree) provides a satisfactory reference for the CASPT2 perturbational treatment of the valence 3d shell in first-row TM systems.

This conclusion changes, however, when considering (3s3p) correlation. With MRCI, Δ_{sp} is always negative, varying between -1 and -6.5 kcal/mol. As compared to the free ions (Table 1) the (3s3p) correlation effect is systematically smaller by a few kcal/mol, but it has the same sign. The same observation holds for NEVPT2, although here Δ_{sp} vanishes or even becomes slightly positive for TM with five or more d electrons. Strikingly though, Δ_{sp} is always positive with CASPT2, reaching values of more than $+5$ kcal/mol for transitions involving a double spin flip. As opposed to the free metal ions, including (3s3p) correlation in standard ($\epsilon = 0.25$ hartree) CASPT2 destabilizes low-spin with respect to high spin states when the ions are surrounded by point charges. As the effect is opposite with MRCI, this gives rise to large discrepancies, more than 10 kcal/mol, between the relative energies obtained from the full CASPT2 and full MRCI treatments. Obviously, the standard CASPT2 zeroth-order Hamiltonian does not provide a satisfactory description of (3s3p) correlation effects in these TM/PC systems, and this causes a systematic over-stabilization of high-spin with respect to low-spin states.

Plots of the CASPT2 spin state energetics as a function of the IPEA shift in the zeroth-order Hamiltonian are presented in Figure 3 for a number of representative cases: FeX_6 , FeX_4 , and NiX_4 . These figures include both CASPT2($n_e,5$) and CASPT2($n_e,10$) results, and show the relative spin state energies obtained from calculations with and without (3s3p) correlation. Considering first

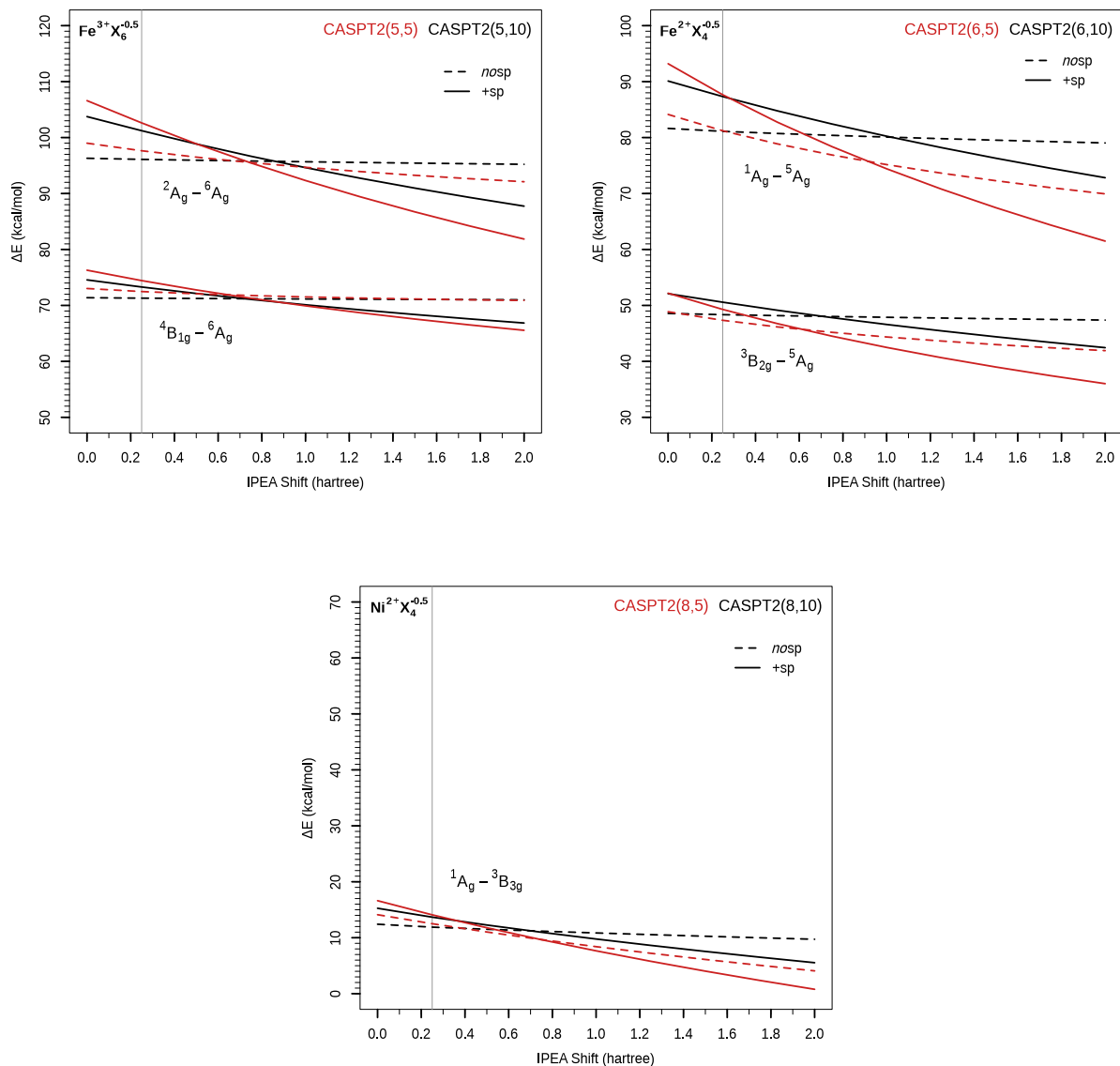


Figure 3: Spin state energetics as a function of the IPEA shift in the CASPT2 zeroth-order Hamiltonian: Fe^{3+}X_6 , Fe^{2+}X_4 , and Ni^{2+}X_4 .

the valence only results, the difference in behaviour between $\text{CASPT2}(n_e, 5)$ and $\text{CASPT2}(n_e, 10)$ is noteworthy. When based on an active space consisting of the five 3d orbitals only, the valence CASPT2 spin state energetics are IPEA-dependent, with relative energies (with respect to the highest spin state) that decrease with increasing ϵ . However, this dependence can be reduced to virtually zero by extending the active space with a second d-shell, i.e. by describing the double-shell

effect in the reference wave function. This improvement in behaviour is general for all considered first-row TM systems (see Figure S2–S6). It is also illustrated by the numbers obtained for the slope $\delta\Delta E$ of the $\Delta E(nosp)$ results in Table 2 (and Tables S3–S5). $\delta\Delta E$ is defined in eq. 2 and is shown in parentheses next to the respective CASPT2 energies. With CASPT2($n_e,5$) negative slopes ranging between 1.1 and 5.1 (kcal/mol)(hartree)⁻¹ are found for transitions involving a single spin flip, and between 5.1 and 7.1 (kcal/mol)(hartree)⁻¹ for a double spin flip. In CASPT2($n_e,10$) these numbers are strongly reduced in all cases, to at most 1.3 (kcal/mol)(hartree)⁻¹.

Much steeper $\Delta E-\epsilon$ curves are obtained when including (3s3p) correlation in the CASPT2 treatment. Noteworthy is that $\delta\Delta_{sp}$, i.e. the ‘extra’ negative slope in the $\Delta E-\epsilon$ curves caused by (3s3p) correlation (shown in parentheses next to the CASPT2 Δ_{sp} results in Table 2) are not so much dependent on the specific TM/PC combination as they are on the number of electrons involved in the spin transition. The CASPT2($n_e,10$) results show slopes in Δ_{sp} of -3.4 to -4.4 (kcal/mol)(hartree)⁻¹ when the total spin changes with only one unit, and almost double, -7.4 to -8.2 (kcal/mol)(hartree)⁻¹ when two electrons change spin. In these calculations, ϵ might therefore be used as a variable that can be increased to produce more accurate CASPT2 relative state energies. However, considering that the standard CASPT2 $\Delta E(+sp)$ values may differ from MRCI by more than 10 kcal/mol, very large IPEA shifts, 1.5 hartree or larger, would be needed to close the gap between both sets of results.

This is further illustrated by Figure 4, showing the progression of the ${}^4B_{1g}-{}^6A_g$ relative energy in $Fe^{3+}X_6$ with the Fe–point charge distance at the CASPT2 (with different ϵ) and MRCI levels, either without (left) or with (right) (3s3p) correlation. Figure 4 clearly shows that without (3s3p) correlation the CASPT2 plots very closely follow the MRCI curve, independently of ϵ . After including (3s3p) correlation, this is no longer the case, at least not for the curves obtained with small ϵ values. With MRCI, the $\Delta E(+sp)$ curve consistently remains below the $\Delta E(nosp)$ curve, that is Δ_{sp} is negative at all distances. With standard CASPT2, however, the effect of (3s3p) correlation goes from negative to positive when the PC are moved closer to the metal. The faulty description of (3s3p) correlation at low ϵ values is further demonstrated by the quartet-sextet relative energy

$\Delta E(+sp)$, which initially increases as the point charges are moved closer to the metal. Such a behaviour is physically incorrect (cfr. the Tanabe-Sugano diagrams), because increasing the crystal field strength $10Dq$ should necessarily stabilize (with respect to the free ion) any d–d transition involving an $e_g \rightarrow t_{2g}$ de-excitation. This figure also illustrates how the CASPT2 description may be improved by increasing the value of the IPEA shift. However, to match the MRCI curve, a very large IPEA shift (around 1.6 hartree at 1.1 Å) is required.

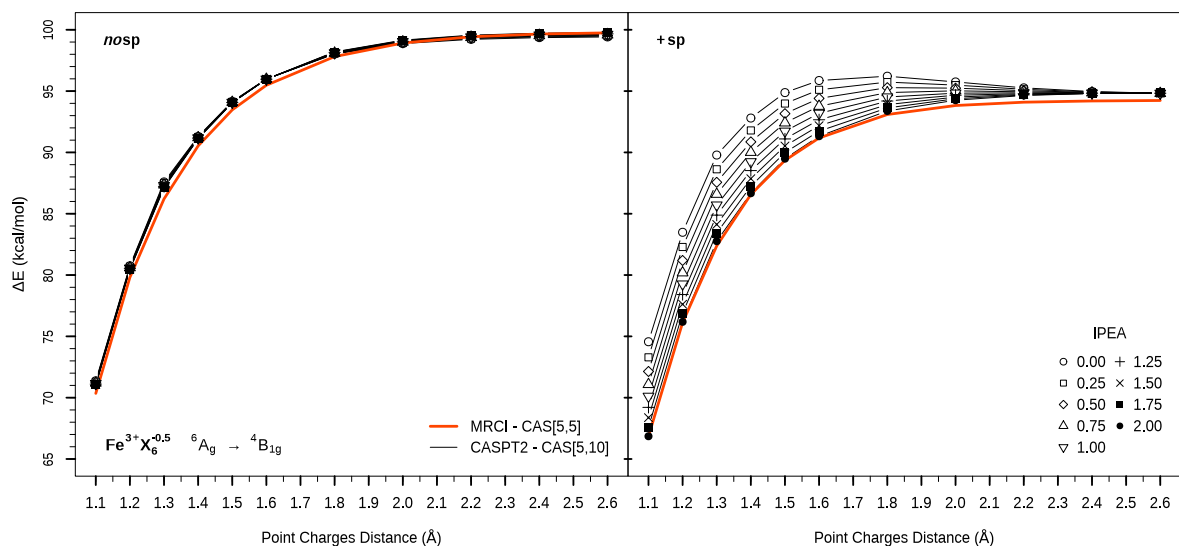


Figure 4: ${}^6A_g \rightarrow {}^4B_{1g}$ energy $Fe^{3+}X_6$ obtained from MRCI and from CASPT2 with different values of ϵ , as a function of the Fe–PC distance.

Spin state energetics in first-row TM molecules

Armed with the information from the previous section we can study the effect of (3s3p) correlation on the spin state energetics in molecular systems and investigate the role of ϵ in the CASPT2 treatment. The molecules chosen for this purpose were introduced at the end of the Introduction and are shown in Figure 1. Calculations on low-lying states with different spin multiplicities were performed with CASPT2, NEVPT2, CCSD, and CCSD(T). The principal electronic configurations of all considered states are provided in Table S2, which also includes a list of criteria to judge the multiconfigurational character of each state, and hence the accuracy to be expected

from CCSD(T). In a benchmark study by Jiang et al.⁶⁸ the following (rough) diagnostic criteria for reliable energetics of CCSD(T) calculations for transition metal compounds were proposed: $T_1 < 0.05$, $D_1 < 0.15$, and $|\%TAE| < 10$, with T_1 and D_1 representing the Frobenius norm and matrix 2-norm of the coupled-cluster amplitudes for single excitations, respectively, and $|\%TAE|$ standing for the percentage of (T) contribution to the total atomization energy. We start by noting that both the T_1 and $|\%TAE|$ criteria are met by all considered complexes, while the D_1 criterion is violated only in a few cases, being the (S=0) state of NiCp(acac), and the (S=1/2), (S=3/2) states of the FeL₂OH, FeL₂OH(NH)₃, and FeL₂SH. Inspection of its CASSCF wave function may provide additional information concerning the multireference character of each state. To be convincingly single reference, the weight of the leading configuration in the CASSCF wave function should be dominant (> 90%), and no other configuration state function (CSF) should appear with a significant (> 2%) weight. The latter can also be verified from the populations of the natural orbitals (NO), which should preferably deviate by less than 0.05 from their formal (Hartree-Fock) values. In transition metal complexes two sources of multiconfigurational effects may be distinguished: (a) Near-degeneracies: if (part of) the metal 3d orbitals are close-lying, this may also be the case for different states belonging to the dⁿ manifold. Such near-degeneracies may lead to failure of single-reference methods. This is precisely why MRCI rather than CCSD(T) was used above for describing the TM ions and the weak field TM/PC systems. As indicated by Table S2, near-degeneracies also occur in some of the molecules, e.g. for the ⁴B_{1g} states in the pseudo-octahedral [Co(NCH)₆]²⁺ complex and in the four-coordinated porphyrins. In the latter molecules, only one orbital (d_{xy}) is destabilized by σ interaction with the porphyrin N, while the other four 3d orbitals remain close-lying. This leads to strong near-degeneracies in e.g. the low-spin (S=1/2) states of MnL₂ and MnP. (b) Left-right correlation: In complexes with strongly covalent metal 3d-ligand bonds an important contribution to the CASSCF wave function originates from CSFs involving electron transfer from the bonding to the antibonding metal 3d-ligand combinations.^{28,44} As there are many such CSFs with small contributions, the CASSCF wave function still keeps only one leading CSF, but with a considerably reduced weight. At the same time, the number of electrons in

the predominantly 3d NOs is significantly increased with respect to their formal occupation number (or decreased in case of π -acceptor ligands). Examples of strong covalent metal ligand bonds in this work are the Fe–OH and Fe–SH bond in the Fe^{III} heme complexes and the M–Cp bond in Mn(Cp)₂ and NiCp(acac). As indicated by the data in Table S2, the weight of the principal configuration in the CASSCF wave function systematically decreases with its spin quantum number, while the D_1 norm shows a concomitant increase. This unbalance in multiconfigurational character between low-spin and high-spin states might of course to some extent affect the accuracy of the CCSD(T) prediction of their relative energy. However, as we shall see below (based on the comparison with CASPT2 and experiment) apart from a few exceptional cases we have no reason to doubt the general quality of the CCSD(T) results obtained in this work. These results will therefore be used as a reference to check the accuracy of the other methods.

Experimental data concerning relative spin state energetics in these molecules are scarce, and in most cases limited to the characterization of the ground state spin multiplicity. Thus, of the four-coordinates metal porphyrins MnP has a high spin (sextet), FeP an intermediate spin (triplet) and CoP a low spin (doublet) ground state.^{69–73} The experimental data for the ferric form of P450, modeled here by FeP(SH), point to a thermal equilibrium between a close-lying doublet and sextet, with a higher-lying quartet state.^{18,74} More precise information concerning the actual electronic energy differences is available for the two organometallic complexes, Mn(Cp)₂ and Ni(Cp)(acac), showing spin crossover behaviour. Here, the difference of electronic energy between the involved spin states may be obtained from the spin crossover temperature $T_{1/2}$, and was estimated to be 1.7 kcal/mol for the singlet→triplet transition in Me₅C₅Ni(acac) ($T_{1/2}$ = 303 K in C₆H₆⁷⁵), and 3.6 kcal/mol for the doublet→sextet transition in manganocene ($T_{1/2}$ = 212 K in toluene).⁴⁷

The calculated relative energies with the four methods CCSD, CCSD(T), NEVPT2 and CASPT2, either with or without (3s3p) correlation, are collected in Table 3, while Figure 5 shows the differences in $\Delta E(nosp)$, $\Delta E(+sp)$, and Δ_{sp} between the other methods and CCSD(T). All relative energies are with respect to the highest possible spin state in each molecule (also where this is not the ground state). The slope of the CASPT2 data, as defined in equations 2 and 3 are also given in

Table 3, in parentheses next to the CASPT2 results obtained with $\epsilon = 0.25$ hartree.

Table 3: Spin state energetics in all molecules considered in this work. Relative spin state energy ΔE (kcal/mol) obtained from different computational approaches

			CCSD	CCSD(T)	NEVPT2	CASPT2 ^a
Mn ^{II} L ₂	⁶ A _g → ⁴ B _{1g}	$\Delta E(nosp)$	23.8	18.2	21.7	19.4(−1.2)
		$\Delta E(+sp)$	20.8	14.1	15.0	16.6(−4.9)
		Δ_{sp}	−3.0	−4.1	−6.7	−2.8(−3.7)
	⁶ A _g → ⁴ B _{3g}	$\Delta E(nosp)$	24.1	13.6	20.5	14.7(−0.3)
		$\Delta E(+sp)$	21.2	9.4	11.6	9.4(−3.6)
		Δ_{sp}	−2.9	−4.2	−8.9	−5.3(−3.3)
	⁶ A _g → ² B _{2g}	$\Delta E(nosp)$	56.0	44.2	53.7	50.7(−2.7)
		$\Delta E(+sp)$	51.9	38.4	44.0	47.8(−10.6)
		Δ_{sp}	−4.1	−5.8	−9.7	−2.9(−7.9)
	⁶ A _g → ² A _g	$\Delta E(nosp)$	53.2	37.7	51.7	46.5(−3.3)
		$\Delta E(+sp)$	49.5	32.3	41.6	43.2(−11.3)
		Δ_{sp}	−3.7	−5.4	−10.1	−3.3(−8.0)
Mn ^{II} P	⁶ A _{1g} → ⁴ A _{2g}	$\Delta E(nosp)$	20.8	17.0	23.5	18.5(−2.8)
		$\Delta E(+sp)$	18.2	13.7	18.4	17.7(−6.4)
		Δ_{sp}	−2.6	−3.3	−5.1	−0.8(−3.6)
	⁶ A _{1g} → ⁴ E _g	$\Delta E(nosp)$	26.9	20.1	39.7	23.0(−2.2)
		$\Delta E(+sp)$	24.0	16.4	32.3	19.9(−5.6)
		Δ_{sp}	−2.9	−3.7	−7.4	−3.1(−3.4)
	⁶ A _{1g} → ² E _g	$\Delta E(nosp)$	60.7	53.7	64.5	56.5(−4.3)
		$\Delta E(+sp)$	57.4	49.2	56.6	55.5(−11.3)
		Δ_{sp}	−3.3	−4.5	−7.9	−1.0(−7.0)
	⁶ A _{1g} → ² B _{1g}	$\Delta E(nosp)$	63.5	56.0	76.9	59.9(−4.3)
		$\Delta E(+sp)$	61.1	52.6	68.7	59.0(−11.0)
		Δ_{sp}	−2.4	−3.4	−8.1	−0.9(−6.7)
Fe ^{II} L ₂	⁵ A _g → ³ B _{1g}	$\Delta E(nosp)$	5.5	−0.6	1.8	0.5(−2.7)
		$\Delta E(+sp)$	2.7	−4.2	−3.2	−1.0(−6.2)
		Δ_{sp}	−2.8	−3.6	−5.0	−1.5(−3.5)

Continued on next page

Continuation from previous page

		CCSD	CCSD(T)	NEVPT2	CASPT2 ^a		
	${}^5A_g \rightarrow {}^3B_{3g}$	$\Delta E(nosp)$	3.8	-3.5	1.8	-1.6(-3.2)	
		$\Delta E(+sp)$	1.4	-6.8	-3.0	-3.0(-6.9)	
		Δ_{sp}	-2.4	-3.3	-4.8	-1.4(-3.7)	
	${}^5A_g \rightarrow {}^1A_g$	$\Delta E(nosp)$	40.7	34.2	33.2	36.1(-6.9)	
		$\Delta E(+sp)$	39.7	32.4	29.3	40.0(-14.7)	
		Δ_{sp}	-1.0	-1.8	-3.9	+3.8(-7.8)	
	Fe ^{II} P	${}^5A_{1g} \rightarrow {}^3A_{2g}$	$\Delta E(nosp)$	8.4	3.7	8.7	5.1(-3.9)
			$\Delta E(+sp)$	5.9	0.6	4.7	4.8(-7.5)
			Δ_{sp}	-2.5	-3.1	-4.0	-0.3(-3.6)
${}^5A_{1g} \rightarrow {}^3E_g$		$\Delta E(nosp)$	9.6	5.1	13.1	6.8(-3.2)	
		$\Delta E(+sp)$	7.4	2.3	9.7	7.0(-8.4)	
		Δ_{sp}	-2.2	-2.8	-3.4	+0.2(-3.7)	
${}^5A_{1g} \rightarrow {}^1A_{1g}$		$\Delta E(nosp)$	39.6	34.3	41.8	36.0(-7.9)	
		$\Delta E(+sp)$	39.0	33.0	39.5	39.9(-15.2)	
		Δ_{sp}	-0.6	-1.3	-2.3	+3.9(-7.3)	
Co ^{II} L ₂		${}^4A_g \rightarrow {}^4B_{2g}$	$\Delta E(nosp)$	-0.3	-0.8	0.4	-0.8(-0.1)
			$\Delta E(+sp)$	-0.3	-0.7	0.3	-0.8(-0.2)
			Δ_{sp}	0.0	0.0	-0.1	0.0(-0.1)
	${}^4A_g \rightarrow {}^2A_g$	$\Delta E(nosp)$	-1.8	-8.7	-4.2	-7.6(-4.8)	
		$\Delta E(+sp)$	-3.0	-10.6	-7.2	-7.7(-8.1)	
		Δ_{sp}	-1.2	-1.9	-3.0	-0.1(-3.3)	
	${}^4A_g \rightarrow {}^2B_{3g}$	$\Delta E(nosp)$	-3.1	-14.5	-5.5	-12.4(-3.2)	
		$\Delta E(+sp)$	-5.1	-17.4	-11.1	-15.1(-7.6)	
		Δ_{sp}	-2.0	-2.9	-5.6	-2.7(-4.4)	
	Co ^{II} P	${}^4B_{1g} \rightarrow {}^4E_g$	$\Delta E(nosp)$	0.6	0.9	1.4	0.7(-0.3)
			$\Delta E(+sp)$	0.7	0.9	1.6	0.9(-0.4)
			Δ_{sp}	0.1	0.0	+0.2	+0.2(-0.1)
${}^4B_{1g} \rightarrow {}^2A_{1g}$		$\Delta E(nosp)$	0.9	-4.2	5.2	-1.7(-5.6)	
		$\Delta E(+sp)$	-0.6	-6.3	2.8	-0.9(-8.9)	
		Δ_{sp}	-1.5	-2.1	-2.4	+0.8(-3.3)	

Continued on next page

Continuation from previous page

		CCSD	CCSD(T)	NEVPT2	CASPT2 ^a	
	${}^4B_{1g} \rightarrow {}^2E_g$	$\Delta E(nosp)$	7.8	0.5	9.9	2.2(-4.0)
		$\Delta E(+sp)$	6.2	-1.8	6.0	0.8(-6.7)
		Δ_{sp}	-1.6	-2.3	-3.9	-1.4(-2.7)
Fe ^{III} L ₂ OH	${}^6A' \rightarrow {}^4A''$	$\Delta E(nosp)$	19.5	12.2	9.7	11.2(-3.6)
		$\Delta E(+sp)$	15.5	7.2	2.6	8.2(-6.5)
		Δ_{sp}	-4.0	-5.0	-7.1	-3.1(-2.9)
	${}^6A' \rightarrow {}^2A''$	$\Delta E(nosp)$	28.8	13.6	14.1	15.8(-8.3)
		$\Delta E(+sp)$	23.3	6.7	2.3	12.2(-14.9)
		Δ_{sp}	-5.5	-6.9	-11.8	-3.6(-6.6)
Fe ^{III} POH	${}^6A' \rightarrow {}^4A''$	$\Delta E(nosp)$	<i>b</i>	<i>b</i>	15.8	16.0(-4.3)
		$\Delta E(+sp)$	<i>b</i>	<i>b</i>	9.4	13.7(-7.3)
		Δ_{sp}	<i>b</i>	<i>b</i>	-6.4	-2.3(-2.9)
	${}^6A' \rightarrow {}^2A''$	$\Delta E(nosp)$	<i>b</i>	<i>b</i>	26.8	22.8(-9.6)
		$\Delta E(+sp)$	<i>b</i>	<i>b</i>	16.3	20.6(-16.2)
		Δ_{sp}	<i>b</i>	<i>b</i>	-10.5	-2.2(-6.6)
Fe ^{III} L ₂ (NH ₃)OH	${}^6A' \rightarrow {}^4A''$	$\Delta E(nosp)$	24.4	17.1	13.6	16.3(-3.4)
		$\Delta E(+sp)$	20.3	12.0	6.6	13.5(-6.2)
		Δ_{sp}	-4.1	-5.1	-7.0	-2.8(-3.4)
	${}^6A' \rightarrow {}^2A''$	$\Delta E(nosp)$	13.3	-0.9	-1.6	1.1(-8.2)
		$\Delta E(+sp)$	7.6	-8.1	-13.9	-2.7(-14.9)
		Δ_{sp}	-5.7	-7.2	-12.3	-3.9(-6.7)
Fe ^{III} P(NH ₃)OH	${}^6A' \rightarrow {}^4A''$	$\Delta E(nosp)$	<i>b</i>	<i>b</i>	15.5	17.7(-4.1)
		$\Delta E(+sp)$	<i>b</i>	<i>b</i>	9.6	16.0(-7.0)
		Δ_{sp}	<i>b</i>	<i>b</i>	-5.9	-1.7(-2.9)
	${}^6A' \rightarrow {}^2A''$	$\Delta E(nosp)$	<i>b</i>	<i>b</i>	5.6	4.6(-9.6)
		$\Delta E(+sp)$	<i>b</i>	<i>b</i>	-4.8	2.8(-16.4)
		Δ_{sp}	<i>b</i>	<i>b</i>	-10.4	-1.8(-6.8)
Fe ^{III} L ₂ SH	${}^6A' \rightarrow {}^4A''$	$\Delta E(nosp)$	14.5	7.0	2.0	4.2(-4.6)
		$\Delta E(+sp)$	10.8	2.4	-4.2	1.7(-7.7)
		Δ_{sp}	-3.7	-4.6	-6.2	-2.5(-3.3)

Continued on next page

Continuation from previous page

		CCSD	CCSD(T)	NEVPT2	CASPT2 ^a	
	${}^6A' \rightarrow {}^2A''$	$\Delta E(nosp)$	17.3	-0.1	-4.6	-2.6(-11.3)
		$\Delta E(+sp)$	12.0	-6.7	-16.7	-7.2(-17.6)
		Δ_{sp}	-5.3	-6.6	-12.1	-4.6(-6.3)
Fe ^{III} PSH	${}^6A' \rightarrow {}^4A''$	$\Delta E(nosp)$	<i>b</i>	<i>b</i>	10.6	9.6(-5.3)
		$\Delta E(+sp)$	<i>b</i>	<i>b</i>	4.9	8.0(-8.5)
		Δ_{sp}	<i>b</i>	<i>b</i>	-5.7	-1.6(-3.2)
	${}^6A' \rightarrow {}^2A''$	$\Delta E(nosp)$	<i>b</i>	<i>b</i>	14.0	7.4(-14.0)
		$\Delta E(+sp)$	<i>b</i>	<i>b</i>	3.0	4.2(-20.1)
		Δ_{sp}	<i>b</i>	<i>b</i>	-11.0	-3.2(-6.1)
[Fe ^{II} (NCH) ₆] ²⁺	${}^5A_g \rightarrow {}^1A_g$	$\Delta E(nosp)$	21.7	9.9	21.7	8.0(-4.8)
		$\Delta E(+sp)$	18.9	5.5	13.6	7.3(-12.2)
		Δ_{sp}	-2.8	-4.4	-8.1	-0.7(-7.4)
[Co ^{II} (NCH) ₆] ²⁺	${}^4B_{1g} \rightarrow {}^2A_g$	$\Delta E(nosp)$	18.8	13.6	25.4	16.2(-3.3)
		$\Delta E(+sp)$	16.9	10.8	21.0	16.1(-7.0)
		Δ_{sp}	-1.9	-2.8	-4.4	-0.1(-3.7)
Mn ^{II} Cp ₂	${}^6A'_1 \rightarrow {}^2E'_2$	$\Delta E(nosp)$	22.2	7.3	4.6	0.8(-4.4)
		$\Delta E(+sp)$	16.7	-0.5	-6.2	-5.2(-11.7)
		Δ_{sp}	-5.5	-7.8	-10.8	-6.0(-7.3)
Ni ^{II} Cp(acac)	${}^3A'' \rightarrow {}^1A'$	$\Delta E(nosp)$	8.5	0.5	<i>b</i>	-0.5(-8.3)
		$\Delta E(+sp)$	6.9	-1.7	<i>b</i>	-0.9(-10.5)
		Δ_{sp}	-1.6	-2.2	<i>b</i>	-0.5(-2.2)

^aThe numbers within parentheses are the slopes of the respective properties ($\delta\Delta E(nosp)$, $\delta\Delta E(+sp)$, $\delta\Delta_{sp}$) with respect to ϵ , as defined in eqs 2 and 3 (units are (kcal/mol)(hartree)⁻¹)

^bComputationally too expensive

Considering first the valence only results in Table 3, we start by noting the close correspondence between CASPT2 and CCSD(T): with a few exceptions, relative energies obtained with both methods agree to within 3 kcal/mol, and in many cases even to within 2 kcal/mol or less. Excep-

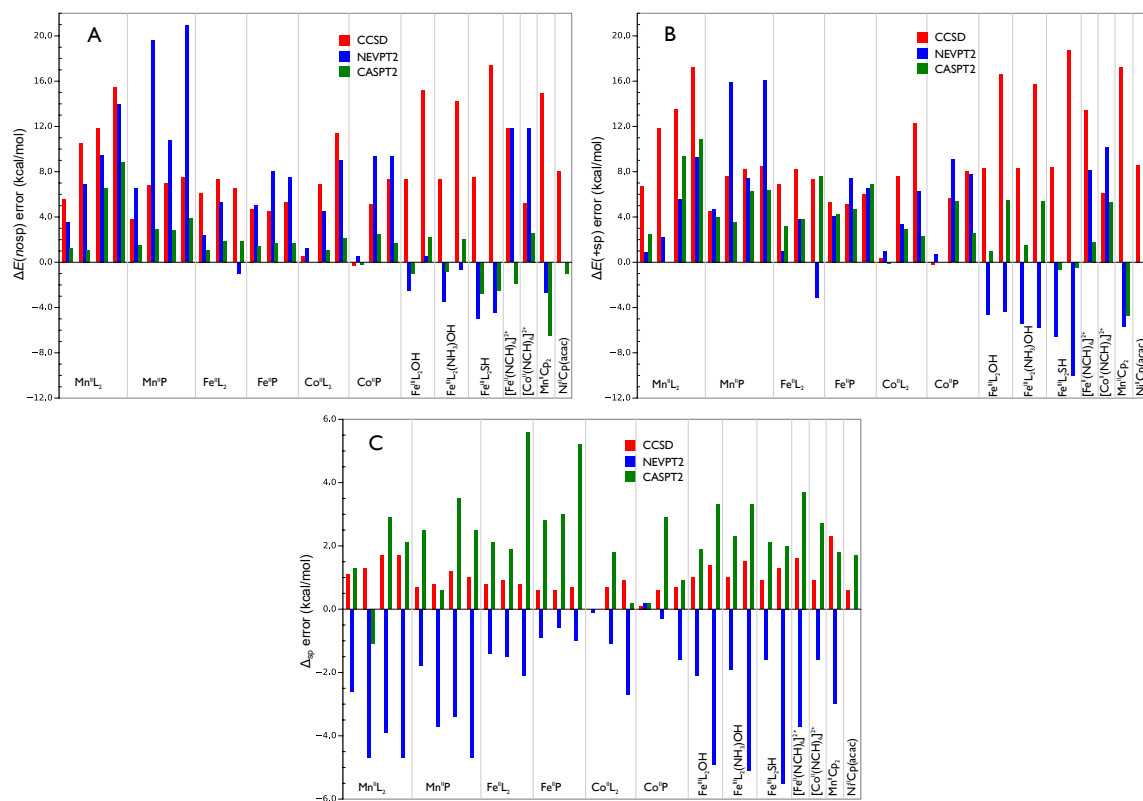


Figure 5: Differences with respect to CCSD(T) of the results obtained with the methods CCSD, NEVPT2 and CASPT2 for the relative spin energetics in different TM molecules: (A) valence only correlation ($\Delta E(nosp)$); (B) full correlation ($\Delta E(+sp)$); (C) (3s3p) correlation effect (Δ_{sp})

tions are found for the ($S = 1/2$)–($S = 5/2$) splittings in the manganese complexes MnL₂, MnP, and Mn(Cp)₂. In the first two cases, some of the CASPT2 energies are considerably higher than the CCSD(T) energies, by up to 9.8 kcal/mol for the 2A_g – 6A_g splitting in MnL₂, while in Mn(Cp)₂ the ${}^2E'_2$ – ${}^6A'_1$ splitting obtained from CASPT2 is lower by 6.5 kcal/mol than the CCSD(T) result. Maybe not unexpectedly, these complexes are amongst the ones showing distinct multiconfigurational effects, at least in their low-spin states, although this is perhaps no reason *per se* to assume that the CCSD(T) results should be inferior to CASPT2. It should also be clear that in all cases, also those that can clearly be marked as single reference, the triples correction is essential to obtain accurate spin state energetics: as Figure 5.A shows, all CCSD energies are systematically too high, by 6.8 kcal/mol (on average) for transitions involving a single spin flip, and 11.6 kcal/mol for transitions involving a double spin flip.

Particularly notable in Table 3 and Figure 5.A are the pronounced differences between the

NEVPT2 and the CCSD(T) results. A general observation (with only a few exceptions) is that where CASPT2 deviates from CCSD(T), NEVPT2 deviates with the same sign but more drastically. For the four-coordinated porphyrin and L_2 systems there is a clear trend in $\Delta E(nosp)$: NEVPT2 \gg CASPT2 $>$ CCSD(T), the difference between NEVPT2 and CCSD(T) becoming as large as 21 kcal/mol. For the five-coordinated L_2 complexes, CASPT2 gives lower quartet-sextet splittings than CCSD(T), and NEVPT2 does so even more. For the doublet-sextet splittings the trends are mixed, but here the three methods in fact quite closely agree. Also for the two inorganic complexes $[\text{Fe}(\text{NCH})_6]^{2+}$ and $[\text{Co}(\text{NCH})_6]^{2+}$ NEVPT2 seems to grossly overestimate the relative energy of the LS with respect to the HS state. Only for the ${}^2E'_2-{}^6A'_1$ splitting $\text{Mn}(\text{Cp})_2$, the NEVPT2 result is significantly closer to CCSD(T) than the CASPT2 result. These results are in a marked contrast to the results from the previous sections, where we found that valence only CASPT2 and NEVPT2 give close-lying results, which are also close to MRCI.

Next, we consider the effect of (3s3p) correlation. At the CCSD(T) level, Δ_{sp} is systematically negative, ranging between -2 and -8 kcal/mol. This conforms to what we found with MRCI for the free TM ions and for the TM ions in a field of point charges, and confirms the crucial role of (3s3p) correlation for accurate relative spin state energetics in TM complexes. Without the triples correction, CCSD still predicts a negative Δ_{sp} , although it is systematically a little smaller ($1-2$ kcal/mol in absolute value) than with CCSD(T). Contrary to what was observed for the TM/PC systems, CASPT2 now also almost invariably predicts a negative effect of (3s3p) correlation on the relative energies in Table 3 (a notable exception being the singlet-quintet splitting in FeL_2 and FeP , for which CASPT2 still predicts a positive Δ_{sp}). However, in virtually all cases the CASPT2 relative energy decrease caused by (3s3p) correlation is significantly smaller than with CCSD and more so than with CCSD(T). Even if the difference in Δ_{sp} between CASPT2 and CCSD(T) amounts to no more than $3-4$ kcal/mol in most cases (Figure 5.B), this is enough to produce final CASPT2 energy splittings $\Delta E(+sp)$ that are higher than the corresponding CCSD(T) values in all but two cases ($\text{Mn}(\text{Cp})_2$ and FeL_2SH ; Figure 5.B). This proves that full CASPT2 indeed systematically overstabilizes high spin with respect to lower spin states, an observation that was already made before

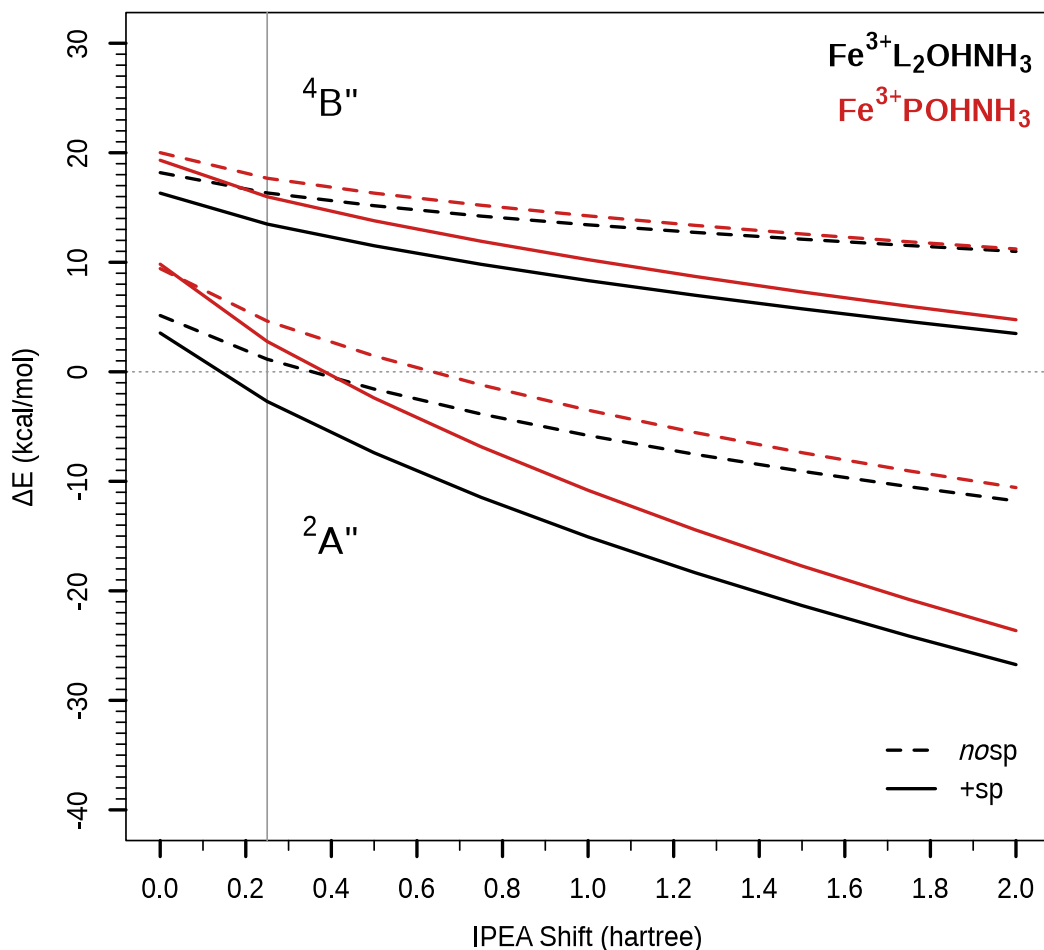


Figure 6: Spin state energetics as a function of the IPEA shift in the CASPT2 zeroth-order Hamiltonian using a CAS(11,15): (black) $\text{FeL}_2(\text{NH}_3)(\text{OH})$, (red) $\text{FeP}(\text{NH}_3)(\text{OH})$.

on several occasions^{6,28–33} but was never brought back to the inadequate CASPT2 treatment of (3s3p) correlation. In those cases where valence only CASPT2 already predicted higher $\Delta E(\text{nosp})$ than CCSD(T), e.g. the four-coordinated porphyrin and L_2 molecules, the two differences add up and the relative energies obtained from the full correlation treatment in CASPT2 versus CCSD(T) differ by 5–8 kcal/mol. Such an error is unacceptably large if CASPT2 is to be used for example to describe the involvement of different spin states in bio-inorganic catalysis, spin-crossover behavior, etc. Also striking of course is that both perturbational approaches CASPT2 and NEVPT2

completely disagree in their way of describing (3s3p) correlation, as is nicely demonstrated by Figure 5.C. With NEVPT2, the effect of (3s3p) correlation on the relative spin state energetics is systematically (much) more negative than with CCSD(T). As valence only NEVPT2 predicts too high relative energies in many cases, by compensation of errors this may lead to full NEVPT2 results that are close to CCSD(T), in some cases closer than CASPT2.

An important question that remains to be answered concerns the role of the IPEA shift in the CASPT2 spin state energetics. In Figure 6 the relative spin state energetics as a function of ϵ is shown for two representative molecules: $\text{FeL}_2(\text{NH}_3)(\text{OH})$ and $\text{FeP}(\text{NH}_3)(\text{OH})$. Compact information on all molecules is provided by the ‘slopes’ of the relative energies and Δ_{sp} with respect to ϵ , as defined by Eqs 2 and 3 and provided in Table 3 next to the corresponding CASPT2 data. All slopes are negative, confirming that the IPEA shift serves to stabilize low spin with respect to high spin states. However, as opposed to the situation in the TM ions (free or surrounded by PC) we now find that even without (3s3p) correlation and including a 3d double-shell in the active space, the valence only CASPT2 relative energies $\Delta E(\text{nosp})$ quite strongly depend on the IPEA shift, $\delta\Delta E(\text{nosp})$ ranging between -1.2 to -14.0 (kcal/mol)(hartree) $^{-1}$. Obviously, this dependence is related to the fact that in the molecules, the correlation of most ligand valence electrons is treated in the CASPT2 rather than in the CASSCF step, and is likely to disappear when the active space could be extended to include all valence electrons. As illustrated by Figure 6, and from a comparison between the different transitions in the L_2 and corresponding porphyrin complexes in Table 3, we find that all slopes are systematically (somewhat) larger in the latter complexes. This shows that the dependence of the valence only CASPT2 relative energies on IPEA increases with the number of valence electrons. We also find that the slope of all valence only CASPT2 energies is systematically larger (about double) for transitions where the total spin is lowered by two rather than one unit.

However, the dependence on ϵ of the valence only CASPT2 data should not *a priori* mean that the ‘standard’ ($\epsilon = 0.25$ hartree) results are not trustworthy. Indeed, as discussed above, the valence only CASPT2 results are on average close to CCSD(T), with acceptable differences of

2–3 kcal/mol max between both methods. It would of course be possible to finetune the CASPT2 results for each specific transition by changing ϵ , but the differences shown in Figure 5 suggest that on average an ϵ shift of 0.25 hartree is appropriate, as some of the valence CASPT2 data are too high (i.e. would benefit from a higher ϵ), others are too low (i.e. would benefit from a lower ϵ).

On the other hand, it is clear that the description of (3s3p) correlation in general would benefit from a higher ϵ . In this respect it is worthwhile to compare the slopes in Δ_{sp} ($\delta\Delta_{\text{sp}}$, in parentheses next to the standard CASPT2 values) between the different molecules/states in Table 3 and also with the TM/PC systems in Table 2. For the molecules, $\delta\Delta_{\text{sp}}$ is -3.4 ± 1.2 and -7.0 ± 1.0 (kcal/mol)(hartree) $^{-1}$ for resp. single and double spin flip transitions. The corresponding data for the TM/PC combinations (Table 2) all fall within these ranges. This shows that the problem with the CASPT2 description of (3s3p) correlation essentially remains a metal only problem also in the molecules, only affecting the *core – core* (3s3p)–(3s3p) and *core – valence* (3s3p)–(3d) terms, but not the (3s3p)–ligand correlation terms. However, solving this problem by increasing ϵ cannot be done without simultaneously deteriorating the valence contribution to the relative energies $\Delta E(\text{nosp})$. As the ϵ dependence of the latter contribution quite strongly depends on the specific molecule/transition, it is hardly possible to define a single optimal IPEA shift that could provide accurate CASPT2 spin state energetics in all TM molecules. The only way out might be to implement IPEA shifts in the CASPT2 zeroth-order Hamiltonian that can vary with the specific type of electron excitation.

The question remains whether this problem might not be solved by extending the active space to include the (3s3p) and possibly also a virtual (4s4p) shell ? When using CASSCF to build the reference wave function, this is often hard to realize due to computational constraints limiting the size of the active space. However, with the alternative RASSCF,²² DMRG,^{23–26} or FCIQMC-CASSCF¹¹ approaches much larger active spaces can be used, with the option of including also core orbitals and their (first) virtual counterparts. In this respect, it is worthwhile to mention the results from our previous RASPT2 study on the spin state energetics of FeP. These results are

included in Table 4 (first two lines), collecting some relevant ab initio results for the spin state energetics of this molecule, from this and other recent works.^{18,42} Experimentally, four-coordinate iron^{II} porphyrins have a triplet ground state.^{70–72} Several CASPT2 studies, making use of different active spaces, have been reported in the past.^{28,42,76,77} All of them incorrectly pointed to a quintet ground state. In the older calculations, this is partly because of the lack of IPEA shift and the use of (too) small basis sets.^{28,76,77} In ref. 42 the inaccurate behavior of CASPT2 was linked to an incorrect description of (3s3p) correlation, and it was suggested to include the four semi-core orbitals into the active space. As can be seen from Table 4, $^3A_{2g}$ was indeed found to be the ground state in CASPT2(16,15), including in the active space the (3s3p) orbitals next to the (3d,4d) shells and a bonding P σ orbital. However, two points should be put forward to place this result into the proper perspective. The first point concerns the basis set used in the ref. 42. As was discovered recently,⁵⁷ an erroneous ANO-RCC basis set for C used to be implemented in the MOLCAS basis set library (in all versions spanning 2006–2014). The basis set was replaced recently, and the new C basis set was used in all calculations performed in this work. As was already reported in an extensive test study by Vela et al.³³, the use of the erroneous C basis gives rise to appreciable errors in the CASPT2 spin state energetics for (spin-crossover) TM systems with organic ligands. Moreover, the error is systematically in favor of low spin with respect to high spin states. This is illustrated by the CASPT2 results in Table 4: comparing the CASPT2(8,11) and CASPT2(16,15) results from the present with our previous work,⁴² we observe a systematic stabilization of the $^5A_{1g}$ state with respect to the lower spin states, by 2.7–3.5 kcal/mol. With the correct C basis set, CASPT2(16,15) again points to a quintet ground state. The second point concerns the construction of the (16,15) active space itself, which we feel might be unbalanced as it includes a correlating shell for the 3d, but not for the (3s3p) orbitals.⁷⁸ This is corroborated by the fact that both RASPT2(16,19) and DMRG(16,19)/CASPT2, including also (4s4p) in the active space, give relative state energies that are again closer to CASPT2(8,11). Both PT2(16,19) calculations predict a quintet ground state and the resulting relative energies deviate by 3.7–5.3 kcal/mol from the CCSD(T) results obtained with the same basis set.

These results also indicate an obvious deficiency in the presently used ANO-RCC basis sets (with correct C basis): even with the loose contraction used in this work, these basis sets still show significant errors for spin state energetics. For the complexes MnL_2 , FeL_2 , CoL_2 , FeP , and FeL_2SH , we can directly compare our CCSD(T) results to ref. 18, reporting CCSD(T) spin state energetics obtained from an extrapolation to complete basis set (CBS) (mixed with explicitly correlated (F12) methodology). As compared to these results, the CCSD(T) relative spin state energies in Table 3 are all too high by 2–4 kcal/mol. This is illustrated for FeP in Table 4, showing that in the CBS limit CCSD(T) does predict $^3\text{A}_{2g}$ to become the ground state, lying 2.3 kcal/mol below the quintet state. CCSD(T) calculations extrapolated to the CBS limit have also been performed by Lawson Daku et al.³² for the two complexes $[\text{Fe}^{\text{II}}(\text{NCH})_6]^{2+}$ and $[\text{Co}^{\text{II}}(\text{NCH})_6]^{2+}$. For the $^1\text{A}_g$ – $^5\text{A}_g$ splitting in $[\text{Fe}^{\text{II}}(\text{NCH})_6]^{2+}$ an energy difference of 2.0 kcal/mol was reported, and 8.9 kcal/mol for the $^2\text{A}_g$ – $^4\text{B}_{1g}$ splitting in $[\text{Co}^{\text{II}}(\text{NCH})_6]^{2+}$, again 2–3 kcal/mol lower than the corresponding CCSD(T) results in Table 3, 5.5 and 10.8 kcal/mol respectively. Obviously, in the ANO scheme, even more extensive contractions (or larger primitive sets) are needed to capture the differential (essentially dynamic) correlation effects between HS and LS states in transition metal complexes.

Summary and conclusion

Because the Hartree-Fock (HF) wave function includes Fermi but not Coulomb correlation, all correlated wave function calculations dealing with spin state energetics inevitably start off from a reference wave function that is strongly biased toward high spin states. The CASSCF wave function that replaces HF in the perturbational treatments CASPT2 and NEVPT2 of the TM complexes considered in this work includes important static (left-right) correlation effects involved in the metal-ligand bonds as well as the 3d double-shell effect, but it cannot account for the differential correlation between the different spin states, that is essentially dynamic in nature. The bias towards high spin states in these complexes can only be fully overcome by an elaborate treatment

Table 4: Spin state energetics in FeP: Relative spin state energy ΔE (kcal/mol) obtained from a full correlation treatment with different computational approaches/basis sets

	${}^5A_{1g} \rightarrow {}^3A_{2g}$	${}^5A_{1g} \rightarrow {}^3E_g$	${}^5A_{1g} \rightarrow {}^1A_{1g}$
CASPT2(8,11) ^a	2.1	4.2	37.1
CASPT2(16,15) ^a	-0.9	1.4	36.7
CASPT2(8,11) ^b	4.8	7.0	39.9
CASPT2(16,15) ^b	1.8	4.1	40.2
RASPT2(16,19) ^{b,c}	4.3	6.4	38.3
DMRG(16,19)/CASPT2 ^{b,d}	4.2	6.3	39.4
CCSD(T) ^b	0.6	2.3	33.0
CCSD(T) ^e	-2.3	-0.6	29.9

^aprevious work, using exactly the same computational procedure/basis sets as in this work, except for the old erroneous ANO-RCC basis set for C⁴²

^bthis work, using correct ANO-RCC basis set for C

^cwith (3s3p) in RAS1, (4s4p) in RAS3, other 11 orbitals in RAS2, and allowing up to quadruple excitations out of RAS1 and into RAS3

^dnumber of renormalized states = 1500

^eextrapolated to CBS, from ref. 18

of dynamic correlation in a complete basis set, involving all ligand valence electrons as well the metal 3d valence and (3s3p) semi-core electrons. Any compromise on such a treatment, by cutting back on either the basis set or on the number of correlated electrons, is bound to give remaining errors that are positive (with the highest spin state at zero energy). This is the case, for example, in the valence only MRCI and CCSD(T) calculations presented in this work, producing values of $\Delta E(nosp)$ that are systematically too high by several kcal/mol (up to 10). The difference between $\Delta E(nosp)$ and the relative energy obtained from the full correlation treatment, $\Delta E(+sp)$, is called Δ_{sp} and is always negative.

The primary goal of this study has been to investigate the accuracy obtained from second-order perturbation theory (PT2) for the (3s3p) contribution to the relative spin state energetics Δ_{sp} in first-row TM complexes and, in case of CASPT2, how this contribution is affected by the value of the IPEA shift ϵ . To introduce the problem, we started with two sets of calculations

on the relative term energies in TM ions, either bare or surrounded by a set of point charges representing a (weak) ligand field. In the bare TM ions, a transition between terms with different spin multiplicity merely involves a reorganization of electron spins in the degenerate 3d open shell. On the other hand, when surrounded by point charges, the transition between spin states involves a ligand field transition, that is (de)excitation of one or two electrons between two subsets of 3d-orbitals with a different energy. Provided that the 3d double-shell effect is included in the reference wave function, we find that PT2 with both types of zeroth-order Hamiltonian (and independent of ϵ), performs well for the valence (3d) correlation contribution, producing relative energies that are close to MRCI to within 2 kcal/mol. Striking, however, is the completely different behavior of CASPT2 in describing the effect of (3s3p) correlation in both situations. In the bare TM ions, CASPT2 correctly predicts negative values of Δ_{sp} , close to MRCI, and virtually independent of the IPEA shift. But in a field of point charges, Δ_{sp} values gradually become positive as the PC are moved closer to the metal. At the same time, the full CASPT2 results become strongly dependent on the value of ϵ . At short TM–PC distances (1.1–1.2 Å) the difference in Δ_{sp} between CASPT2 and MRCI may become as large as 12 kcal/mol. The faulty description of (3s3p) correlation with CASPT2 is responsible for a strong overstabilization of higher with respect to lower spin states in the full CASPT2 treatment. Increasing the IPEA shift in the zeroth-order hamiltonian reduces the CASPT2 error. However, to match the full CASPT2 relative energies with MRCI very high ϵ values (> 1.5 hartree) are required. Noteworthy is also that NEVPT2 does succeed in correctly describing the (3s3p) correlation effect both in free and PC surrounded TM ions.

The erratic CASPT2 behavior in describing (3s3p) correlation also remains in the TM molecules (Figure 1), although here the error in Δ_{sp} (with respect to CCSD(T)) is less dramatic than in the TM/PC models. A positive note about CASPT2 is certainly that it works quite well for valence correlation: with a few exceptions (possibly because of multiconfigurational effects deteriorating CCSD(T)), the spin states energetics obtained from the valence only (standard IPEA) CASPT2 calculations are found to be close (to within 3 kcal/mol or less) to CCSD(T). Increasing ϵ might serve to improve the CASPT2 description of (3s3p) correlation, but only at the expense of deteriorating

the description of (system dependent) valence correlation, and is therefore not recommended.

As to our knowledge, the present study also presents the first systematic set of NEVPT2 calculations on spin state energetics in a relevant series of TM complexes. Quite remarkably maybe, our findings concerning this method are not very positive. Large differences (up to 20 kcal/mol) are found in the valence contribution between NEVPT2 on the one hand and CASPT2/CCSD(T) on the other hand (Figure 5.A). Moreover, the (3s3p) correlation contribution Δ_{sp} obtained from NEVPT2 is more often than not even more erratic than with CASPT2, but now systematically too negative (Figure 5.C). In those cases where the resulting full NEVPT2 results are closer to CCSD(T) than CASPT2 (Figure 5.B), this is therefore merely due to a cancellation of errors.

Our final conclusion is that (standard) CASPT2, rather than NEVPT2, still remains the most appropriate PT2 method for treating spin state energetics in TM systems that are either too large or too multiconfigurational to be comfortably treated with CCSD(T). The origin of the systematic overstabilization of high with respect to low spin states by CASPT2, observed in previous studies,^{6,28–33} has in this study been explored in detail, and is primarily attributed to the inappropriate description of (3s3p) correlation. Next to this, basis set insufficiencies, even in the extended ANO basis sets used in this work, are also partly responsible.

Acknowledgement

This investigation has been supported by grants from the Flemish Science Foundation (FWO). The computational resources and services used in this work were provided by the VSC (Flemish Supercomputer Center), funded by the Hercules Foundation and the Flemish Government-department EWI. The COST Action ECOSTBio CM1305 from the European Union is also gratefully acknowledged.

Supporting Information Available

Symmetry information and principal configurations of all considered states in the TM/PC and molecular systems. T_1 , D_1 and $|\%TAE|$ diagnostics for all molecular states. Relative spin state

energetics for TM/PC systems other than the ones included in Table 2. Plot of the natural orbitals of the NiCp(acac) molecule. Cartesian coordinates of all molecules studied in this work. This material is available free of charge via the Internet at <http://pubs.acs.org/>.

References

- (1) Harvey, J. N. *Structure and Bonding* **2004**, *112*, 151–183.
- (2) Harvey, J. N. *Annu. Rep. Prog. Chem., Sect. C: Phys. Chem.* **2006**, *102*, 203–226.
- (3) Ghosh, A. *J. Biol. Inorg. Chem.* **2006**, *11*, 712–724.
- (4) Pierloot, K.; Vancoillie, S. *J. Chem. Phys.* **2006**, *125*, 124303.
- (5) Pierloot, K.; Vancoillie, S. *J. Chem. Phys.* **2008**, *128*, 034104.
- (6) Vancoillie, S.; Zhao, H.; Radoń, M.; Pierloot, K. *J. Chem. Theory Comput.* **2010**, *6*, 576–582.
- (7) Kurashige, Y.; Chalupský, J.; Lan, T. N.; Yanai, T. *J. Chem. Phys.* **2014**, *141*, 174111.
- (8) Eriksen, J. J.; Baudin, P.; Ettenhuber, P.; Kristensen, K.; Kjærgaard, T.; Jørgensen, P. *J. Chem. Theory Comput.* **2014**, *11*, 2984–2993.
- (9) Saitow, M.; Kurashige, Y.; Yanai, T. *J. Chem. Theory Comput.* **2015**, *11*, 5120–5131.
- (10) Liakos, D. G.; Neese, F. *J. Chem. Theory Comput.* **2015**, *11*, 4054–4063.
- (11) Li Manni, G.; Smart, S. D.; Alavi, A. *J. Chem. Theory Comput.* **2016**, *12*, 1245–1258.
- (12) Ma, D.; Li Manni, G.; Olssen, J.; Gagliardi, L. *J. Chem. Theory Comput.* **2016**, *12*, 3208–3213.
- (13) Knecht, S.; Hedegård, E. D.; Keller, S.; Kovyshin, A.; Ma, Y.; Muolo, A.; Stein, C. J.; Reiher, M. *CHIMIA* **2016**, *70*, 244–251.
- (14) Wouters, S.; Van Speybroeck, V.; Van Neck, D. *J. Chem. Phys.* **2016**, *145*, 054120.
- (15) Freitag, L.; Knecht, S.; Angeli, C.; Reiher, M. *ArXiv e-prints* **2016**, arXiv:1608.02006.
- (16) Knowles, P. J.; Hampel, C.; Werner, H. J. *J. Chem. Phys.* **1993**, *99*, 5219.
- (17) Watts, J. D.; Gauss, J.; Bartlett, R. J. *J. Chem. Phys.* **1993**, *98*, 8718.

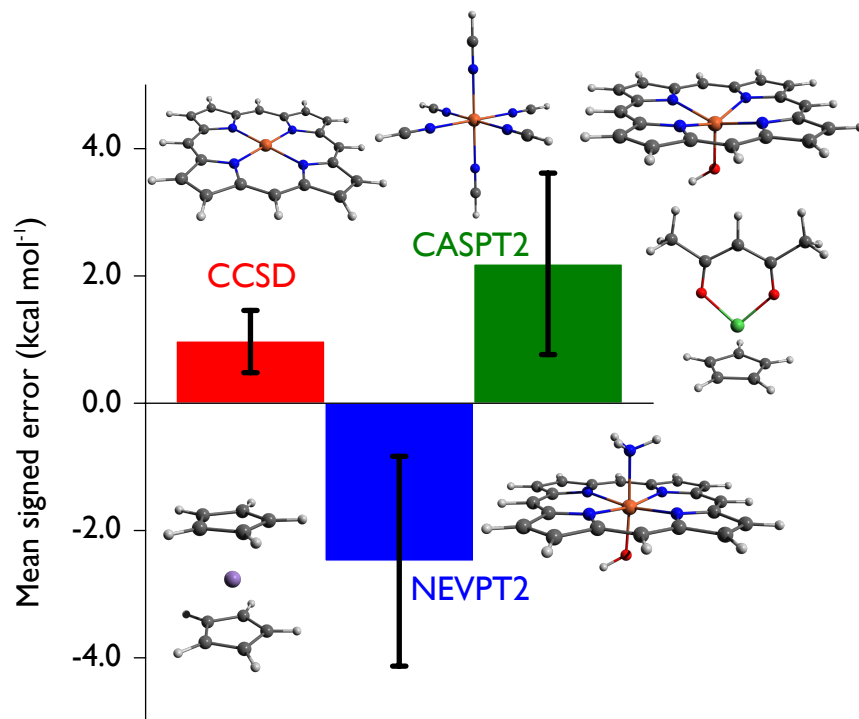
- (18) Radoń, M. *J. Chem. Theory Comput.* **2014**, *10*, 2306–2321.
- (19) Andersson, K.; Malmqvist, P.-Å.; Roos, B. O.; Sadlej, A. J.; Wolinski, K. *J. Phys. Chem.* **1990**, *94*, 5483–5488.
- (20) Andersson, K.; Malmqvist, P.-Å.; Roos, B. O. *J. Chem. Phys.* **1992**, *96*, 1218–1226.
- (21) Angeli, C.; Cimiraglia, R.; Evangelisti, S.; Leininger, T.; Malrieu, J.-P. *J. Chem. Phys.* **2001**, *114*, 10252–10264.
- (22) Malmqvist, P.-Å.; Pierloot, K.; Shahi, A. R. M.; Cramer, C. J.; Gagliardi, L. *J. Chem. Phys.* **2008**, *128*, 204109+.
- (23) White, S. R. *Phys. Rev. Lett.* **1992**, *69*, 2863.
- (24) Chan, G. K.-L. *J. Chem. Phys.* **2004**, *120*, 3172–3178.
- (25) Wouters, S.; Van Neck, D. *Eur. Phys. J. D* **2014**, *68*, 1–20.
- (26) Keller, S.; Dolfi, M.; Troyer, M.; Reiher, M. *J. Chem. Phys.* **2015**, *143*, 244118.
- (27) Rudavskiy, A.; Sousa, C.; de Graaf, C.; Havenith, R. W. A.; Broer, R. *J. Chem. Phys.* **2014**, *140*, 184318.
- (28) Pierloot, K. *Mol. Phys.* **2003**, *101*, 2083–2094.
- (29) Radoń, M.; Broclawik, E.; Pierloot, K. *J. Phys. Chem. B* **2010**, *114*, 1518–1528.
- (30) Radoń, M.; Broclawik, E.; Pierloot, K. *J. Chem. Theory Comput.* **2011**, *7*, 898–908.
- (31) Kepenekian, M.; Robert, V.; Guennic, B. L. *J. Chem. Phys.* **2009**, *131*, 114702.
- (32) Lawson Daku, L. M.; Aquilante, F.; Robinson, T. W.; Hauser, A. *J. Chem. Theory Comput.* **2012**, *8*, 4216–4231.
- (33) Vela, S.; Fumanal, M.; Ribas-Arino, J.; Robert, V. *J. Comp. Chem.* **2016**, *37*, 947–953.

- (34) Ghigo, G.; Roos, B. O.; Malmqvist, P.-Å. *Chem. Phys. Lett.* **2004**, *396*, 142–149.
- (35) Andersson, K.; Roos, B. O. *Int. J. Quantum Chem.* **1993**, *45*, 591.
- (36) Roos, B. O.; Andersson, K.; Fülcher, M. P.; Malmqvist, P.-Å.; Serrano-Andrés, L.; Pierloot, K.; Merchán, M. In *Advances in Chemical Physics: New Methods in Computational Quantum Mechanics, Vol. XCIII*; Prigogine, I., Rice, S. A., Eds.; John Wiley & Sons: New York, 1996; pp 219–332.
- (37) Pierloot, K.; Tsokos, E.; Roos, B. O. *Chem. Phys. Lett.* **1993**, *214*, 583–590.
- (38) Pierloot, K.; Praet, E. V.; Vanquickenborne, L. G.; Roos, B. O. *J. Phys. Chem.* **1993**, *97*, 12220–12228.
- (39) Pierloot, K.; Tsokos, E.; Vanquickenborne, L. G. *J. Phys. Chem.* **1996**, *100*, 16545–16550.
- (40) Persson, B. J.; Roos, B. O.; Pierloot, K. *J. Chem. Phys.* **1994**, *101*, 6810–6821.
- (41) Pierloot, K.; Persson, B. J.; Roos, B. O. *J. Phys. Chem.* **1995**, *99*, 3465–3472.
- (42) Vancoillie, S.; Zhao, H.; Tran, V. T.; Hendrickx, M. F. A.; Pierloot, K. *J. Chem. Theory Comput.* **2011**, *7*, 3961–3977.
- (43) Oláh, J.; Harvey, J. N. *J. Phys. Chem. A* **2009**, *113*, 7338–7345.
- (44) Pierloot, K. In *Computational Organometallic Chemistry*; Cundari, T. R., Ed.; Marcel Dekker, Inc.: New York, 2001; pp 123–158.
- (45) Pierloot, K. *Int. J. Quantum Chem.* **2011**, *111*, 3291–3301.
- (46) Veryazov, V.; Malmqvist, P.; Roos, B. O. *Int. J. Quantum Chem.* **2011**, *111*, 3329–3338.
- (47) Phung, Q. M.; Vancoillie, S.; Pierloot, K. *J. Chem. Theory Comput.* **2012**, *8*, 883–892.
- (48) Phung, Q. M.; Wouters, S.; Pierloot, K. *J. Chem. Theory Comput.* **2016**, *12*, 4352–4361.

- (49) Forsberg, N.; Malmqvist, P.-Å. *Chem. Phys. Lett.* **1997**, *274*, 196.
- (50) Angeli, C.; Cimiraglia, R.; Malrieu, J.-P. *J. Chem. Phys.* **2002**, *117*, 9138–9153.
- (51) Aquilante, F.; De Vico, L.; Ferré, N.; Ghigo, G.; Malmqvist, P.-Å.; Neogrady, P.; Pedersen, T. B.; Pitoňák, M.; Reiher, M.; Roos, B. O.; Serrano-Andrés, L.; Urban, M.; Veryazov, V.; Lindh, R. *J. Comput. Chem.* **2010**, *31*, 224–247.
- (52) Werner, H.-J.; Knowles, P. J.; Knizia, G.; Manby, F. R.; Schütz, M. *WIREs Comput. Mol. Sci.* **2012**, *2*, 242–253.
- (53) Wouters, S.; Poelmans, W.; Ayers, P. W.; Van Neck, D. *Comput. Phys. Commun.* **2014**, *185*, 1501–1514.
- (54) Aquilante, F. et al. *J. Comput. Chem.* **2016**, *37*, 506–541.
- (55) Roos, B. O.; Lindh, R.; Malmqvist, P.-Å.; Veryazov, V.; Widmark, P.-O. *J. Phys. Chem. A* **2005**, *109*, 6575–6579.
- (56) Roos, B. O.; Malmqvist, P.-Å. *Phys. Chem. Chem. Phys.* **2004**, *6*, 2919–2927.
- (57) In the beginning of 2015 an error was discovered in the ANO-RCC basis set of C, included in MOLCAS versions 6.4–8.0. The basis set was replaced by a new correct ANO-RCC basis set, which can be found at <http://www.molcas.org/ANO>. All calculations presented in this work were performed with the correct C basis set.
- (58) Widmark, P.-O.; Malmqvist, P.-Å.; Roos, B. O. *Theor. Chim. Acta* **1990**, *77*, 291.
- (59) Reiher, M.; Wolf, A. *J. Chem. Phys.* **2004**, *121*, 10945–10956.
- (60) Aquilante, F.; Malmqvist, P.-Å.; Pedersen, T. B.; Ghosh, A.; Roos, B. O. *J. Chem. Theory Comput.* **2008**, *4*, 694.
- (61) Boström, J.; Delcey, M. G.; Aquilante, F.; Serrano-Andrés, L.; Pedersen, T. B.; Lindh, R. *J. Chem. Theory Comput.* **2010**, *6*, 747–754.

- (62) TURBOMOLE V6.4 2012, a development of University of Karlsruhe and Forschungszentrum Karlsruhe GmbH, 1989-2007, TURBOMOLE GmbH, since 2007; available from <http://www.turbomole.com>.
- (63) Weigend, F.; Ahlrichs, R. *Phys. Chem. Chem. Phys.* **2005**, *7*, 3297–3305.
- (64) Corliss, C.; Sugar, J. *J. Phys. Chem. Ref. Data* **1977**, *6*, 1253–1329.
- (65) Corliss, C.; Sugar, J. *J. Phys. Chem. Ref. Data* **1982**, *11*, 135–241.
- (66) Sugar, J.; Corliss, C. *J. Phys. Chem. Ref. Data* **1981**, *10*, 1097–1174.
- (67) Corliss, C.; Sugar, J. *J. Phys. Chem. Ref. Data* **1981**, *10*, 198–289.
- (68) Jiang, W.; DeYonker, N. J.; Wilson, A. K. *J. Chem. Theory Comput.* **2012**, *8*, 460–468.
- (69) Kirner, J. F.; Reed, C. A.; Scheidt, W. R. *J. Am. Chem. Soc.* **1977**, *99*, 1093–1101.
- (70) Collman, J. P.; Hoard, J. L.; Kim, N.; Lang, G.; Reed, C. A. *J. Am. Chem. Soc.* **1975**, *97*, 2676–2681.
- (71) Goff, H.; La Mar, G. N.; Reed, C. A. *J. Am. Chem. Soc.* **1977**, *99*, 3641–3646.
- (72) Obara, S.; Kashiwagi, H. *J. Chem. Phys.* **1982**, *77*, 3155.
- (73) Madura, P.; Scheidt, R. G. *Inorg. Chem.* **1976**, *15*, 3182–3184.
- (74) Sligar, S. G. *Biochemistry* **1976**, *15*, 5399–5406.
- (75) Smith, M. E.; Andersen, R. A. *J. Am. Chem. Soc.* **1996**, *118*, 11119–11128.
- (76) Choe, Y.-K.; Hashimoto, T.; Nakano, H.; Hirao, K. *Chem. Phys. Lett.* **1998**, *295*, 380–388.
- (77) Choe, Y.-K.; Nakajima, T.; Hirao, K.; Lindh, R. *J. Chem. Phys.* **1999**, *111*, 3837–3844.

(78) Because of the high, D_{2h} , point group of FeP, the Fe s, p, and d orbitals occur in different representations and cannot mix. Our experience with lower symmetry molecules is that it becomes impossible to include (3s3p) in the active space without including also (4s4p). Otherwise, the 4d orbitals will simply rotate out of the active space in favor of 4p. This points to a more important double shell effect for the 3p than for the 3d electrons.



3s3p correlation contribution to relative spin state energies in transition metal complexes, relative to CCSD(T)

Table of Contents - Graphic